

1

2 Fluvial carbon dioxide emission from the Lena River basin during spring flood

3

4 Sergey N. Vorobyev¹, Jan Karlsson², Yuri Y. Kolesnichenko¹, Mikhail A. Korets³,

5 and Oleg S. Pokrovsky^{4,5*}

6

7 ¹*BIO-GEO-CLIM Laboratory, Tomsk State University, Tomsk, Russia*

8 ²*Climate Impacts Research Centre (CIRC), Department of Ecology and Environmental Science, Umeå*
9 *University, Linnaeus väg 6, 901 87 Umeå, Sweden.*

10 ³*V.N. Sukachev Institute of Forest of the Siberian Branch of Russian Academy of Sciences – separated*
11 *department of the KSC SB RAS, Krasnoyarsk, 660036, Russia*

12 ⁴*Geosciences and Environment Toulouse, UMR 5563 CNRS, 14 Avenue Edouard Belin 31400*
13 *Toulouse, France*

14 ⁵*N. Laverov Federal Center for Integrated Arctic Research, Russian Academy of Sciences,*
15 *Arkhangelsk, Russia*

16

17

18 Key words: CO₂, C, emission, permafrost, river, export, landscape, Siberia

19

20 * email: oleg.pokrovsky@get.omp.eu

21

22 **Abstract**

23 Greenhouse gas (GHG) emission from inland waters of permafrost-affected regions is one of the
24 key factors of circumpolar aquatic ecosystem response to climate warming and permafrost thaw. Riverine
25 systems of central and eastern Siberia contribute a significant part of the water and carbon (C) export to
26 the Arctic Ocean, yet their C exchange with the atmosphere remain poorly known due to lack of *in-situ*
27 GHG concentration and emission estimates. Here we present the results of continuous in-situ pCO₂
28 measurements over a 2600-km transect of the Lena River main stem and lower reaches of 20 major
29 tributaries (together representing watershed area of 1,661,000 km², 66% of the Lena's basin), conducted
30 at the peak of the spring flood. The pCO₂ in Lena (range 400-1400 µatm) and tributaries (range 400-1600
31 µatm) remained generally stable (within ca. 20 %) over the night/day period and across the river channels.

32 The pCO₂ in tributaries increased northward with mean annual temperature decrease and permafrost
33 increase; this change was positively correlated with C stock in soil, the proportion of deciduous needle-
34 leaf forest and the riparian vegetation. Based on gas transfer coefficients obtained from rivers of the
35 Siberian permafrost zone ($k = 4.46 \text{ m d}^{-1}$), we calculated CO₂ emission for the main stem and tributaries.
36 Typical fluxes ranged from 1 to 2 g C m⁻² d⁻¹ (>99% CO₂, < 1 % CH₄) which is comparable with CO₂
37 emission measured in Kolyma, Yukon and Mackenzie and permafrost-affected rivers in western Siberia.
38 The areal C emissions from lotic waters of the Lena watershed were quantified via taking into account
39 the total area of permanent and seasonal water of the Lena basin (28,000 km²). Assuming 6 months of
40 the year to be open water period with no emission under ice, the annual C emission from the whole Lena
41 basin is estimated as $8.3 \pm 2.5 \text{ Tg C y}^{-1}$ which is comparable to the DOC and DIC lateral export to the
42 Arctic Ocean.

43

44

45 **Introduction**

46 Climate warming in high latitudes is anticipated to result in mobilization, decomposition and
47 atmospheric release of significant amounts of carbon (C) stored in permafrost soils, providing a positive
48 feedback (Schuur et al. 2015). Permafrost thawing is expected to also increase the lateral C export to
49 rivers and lakes (Frey and Smith, 2005). The exported permafrost C is relatively labile and largely
50 degraded to greenhouse gases (GHG) in recipient freshwaters (e.g. Vonk et al., 2015). As a result,
51 assessment of GHG emission in rivers of permafrost affected regions is crucially important for
52 understanding the high latitude C cycle under various climate change scenarios (Chadburn et al., 2017;
53 Vonk et al., 2019). Among six great Arctic rivers, Lena is most emblematic one, situated chiefly within
54 the continuous permafrost zone and exhibiting the highest seasonal variation in discharge. Over the past
55 two decades, there has been an explosive interest to the Lena River hydrology (Yang et al., 2002;
56 Berezovskaya et al., 2005; Smith and Pavelsky, 2008; Ye et al., 2009; Gelfan et al., 2017; Suzuki et al.,
57 2018), organic C (OC) transport (Lara et al., 1998; Raymond et al., 2007; Semiletov et al., 2011;
58 Goncalves-Araujo et al., 2015; Kutscher et al., 2017; Griffin et al., 2018) and general hydrochemistry

59 (Gordeev and Sidorov, 1993; Cauwet and Sidorov, 1996; Huh et al., 1998a,b; Huh and Edmond, 1999;
60 Wu and Huh, 2007; Kuzmin et al., 2009; Pipko et al., 2010; Georgiadi et al., 2019; Juhls et al., 2020)
61 including novel isotopic approaches for nutrients (Si, Sun et al., 2018) and trace metals such as Li
62 (Murphy et al., 2019) and Fe (Hirst et al., 2020). This interest is naturally linked to the Lena River
63 location within the forested continuous permafrost/taiga zone covered by organic-rich yedoma soil.
64 Under on-going climate warming, the soils of the Lena River watershed are subjected to strong thawing
65 and active (seasonally unfrozen) layer deepening (Zhang et al., 2005) accompanied by overall increase
66 in river water discharge (McClelland et al., 2004; Ahmed et al., 2020), flood intensity and frequency
67 (Gautier et al., 2018). The Lena River exhibits the highest DOC concentration among all great Arctic
68 rivers (i.e., Holmes et al., 2013) which may reflect weak DOC degradation in the water column and
69 massive mobilization of both contemporary and ancient OC to the river from the watershed (Feng et al.,
70 2013; Wild et al., 2019). In contrast to rather limited works on CO₂ and CH₄ emissions from water
71 surfaces of Eastern Siberia (Semiletov, 1999; Denfeld et al., 2013), extensive studies were performed on
72 land, in the polygonal tundra of the Lena River Delta (Wille et al., 2008; Bussman, 2013; Sachs et al.,
73 2008; Kutzbach et al., 2007) and the Indigirka Lowland (van der Molen et al., 2007). Finally, there have
74 been several studies of sediment and particular matter transport by the Lena River to the Laptev Sea
75 (Rachold et al., 1996; Dudarev et al., 2006) together with detailed research of the Lena River Delta
76 (Zubrzycki et al., 2013; Siewert et al., 2016).

77 Surprisingly, despite such extensive research on C transport, storage, and emission in Eastern
78 Siberian landscapes, C emissions of the Lena River main stem and tributaries remain virtually unknown,
79 compared to a relatively good understanding of those in the Yukon (Striegl et al., 2012; Stackpoole et
80 al., 2017), Mackenzie (Horan et al., 2019), Ob (Karlsson et al., 2021; Pipko et al., 2019) and Kolyma
81 (Denfeld et al., 2013). The only available estimates of C emission from inland waters of the Lena basin
82 are based on few indirect (calculated gas concentration and modelled fluxes) snapshot data with very low
83 spatial and temporal resolution (Raymond et al., 2013). Similar to other regions, this introduces
84 uncertainties and cannot adequately capture total regional C emissions (Abril et al., 2015; Denfeld et al.,
85 2018; Park et al., 2018; Klaus et al., 2019; Klaus and Vachon, 2020; Karlsson et al., 2021). In particular,

86 no detailed studies at the peak of spring flood have been performed and the information on various
87 contrasting tributaries of the Lena River remains very limited. As a result, reliable estimations of
88 magnitude and controlling factors of C emission in the Lena River basin are poorly understood. The
89 present work represents a first assessment of CO₂ and CH₄ concentration and fluxes of the main stem
90 and tributaries during the peak of spring flow, via calculating C emission and relating these data to river
91 hydrochemistry and GIS-based landscape parameters. This should allow identifying environmental
92 factors controlling GHG concentration and emission in the Lena River watershed in order to use this
93 knowledge to foresee future changes in C balance of the largest permafrost-affected Arctic river.

94

95 **2. Study Site, Materials and Methods**

96 *2.1. Lena River and its tributaries*

97 The sampled Lena River main stem and 20 tributaries are located along a 2600 km latitudinal
98 transect SW to NE and include watersheds of distinct sizes, geomorphology, permafrost extent, lithology,
99 climate and vegetation (**Fig. 1, S1 A; Table S1**). The total watershed area of the rivers sampled in this
100 work is approximately 1.66 million km², representing 66% of the entire Lena River basin. Permafrost is
101 mostly continuous except some patches of discontinuous and sporadic in the southern part of the Lena
102 basin (Brown et al., 2002). The mean annual air temperatures (MAAT) along the transect ranges from -
103 5 °C in the southern part of the Lena basin to -9 °C in the central part of the basin. The range of MAAT
104 for 20 tributaries is from -4.7 to -15.9 °C. The mean annual precipitation ranges from 350-500 mm y⁻¹ in
105 the southern and south-western part of the basin to 200-250 mm y⁻¹ in the central and northern parts
106 (Chevychelov and Bosikov, 2010). The lithology of the Siberian platform which is drained by the Lena
107 River is highly diverse and includes Archean and Proterozoic crystalline and metamorphic rocks, Upper
108 Proterozoic, Cambrian and Ordovician dolostones and limestones, volcanic rocks of Permo-Triassic age
109 and essentially terrigenous silicate sedimentary rocks of the Phanerozoic. Further description of the Lena
110 River basin landscapes, vegetation and lithology can be found elsewhere (Rachold et al., 1996; Huh et
111 al., 1999a, b; Pipko et al., 2010; Semiletov et al., 2011; Kutscher et al., 2017; Juhls et al., 2020).

112 The peak of annual discharge depends on the latitude (**Fig. 1**) and occurs in May in the south
113 (Ust-Kut) and in June in the middle and low reaches of the Lena River (Yakutsk, Kysyr). From May 29
114 to June 17, 2016, we moved downstream the Lena River by boat with an average speed of 30 km h⁻¹
115 (Gureyev, 2016). As such, we followed the progression of the spring and moved from the southwest to
116 the northeast, thus collecting river water at approximately the same stage of maximal discharge. Note
117 that transect sampling is a common way to assess river water chemistry in extreme environments (Huh
118 and Edmond, 1999; Spence and Telmer, 2005), and generally, a single sampling during high flow season
119 provides the best agreement with time-series estimates (Qin et al., 2006). Regular stops each 80-100 km
120 along the Lena River allowed sampling for major hydrochemical parameters and CH₄ along the main
121 stem. We also moved 500-1500 m upstream of selected tributaries to record CO₂ concentrations for at
122 least 1 h and to sample for river hydrochemistry; see examples of spatial coverage in **Fig. S1 B**. From
123 late afternoon/evening to the next morning, we stopped for sleep but continued to record pCO₂ in the
124 Lena River main stem (15 sites, evenly distributed over the full 2600 km transect) and two tributaries
125 (Aldan and Tuolba).

126

127 *2.2. CO₂ and CH₄ concentrations*

128 Surface water CO₂ concentration was measured continuously, *in-situ* by deploying a portable
129 infrared gas analyzer (IRGA, GMT222 CARBOCAP® probe, Vaisala®; accuracy $\pm 1.5\%$) of two ranges
130 (2 000 and 10 000 ppm). This system was mounted on a small boat in a perforated steel pipe ~0.5 m
131 below water surface. The tube had two necessary opening of different diameter, which allowed free water
132 flow with a constant rate during the moving of the boat. The probe was enclosed within a waterproof and
133 gas-permeable membrane. The key to aqueous deployment of the IRGA sensor is the use of a protective
134 expanded polytetrafluoroethylene (PTFE) tube or sleeve that is highly permeable to CO₂ but
135 impermeable to water (Johnson et al., 2009). The material is available for purchase as a flexible tube that
136 fits over the IRGA sensor (Product number 200-07; International Polymer Engineering, Tempe, Arizona,
137 USA). We also used a copper mesh screen to minimize biofouling effects (i.e., Yoon et al., 2016).
138 However these effects are expected to be low in cold waters of the virtually pristine Lena River and its

139 tributaries. During sampling, the sensor was left to equilibrate in the water for 10 minutes before
140 measurements were recorded.

141 The probe was enclosed and placed into a tube which was submerged 0.5 m below the water
142 surface. Within this tube, we designed a special chamber that allowed low-turbulent water flow around
143 the probe without gas bubbles. Previous studies (Park et al., 2021; Crawford et al. 2015; Yoon et al.,
144 2016) reported some effects of boat speed on sensor CO₂ measurements due to turbulences. Although
145 the turbulences were minimized in the tube/chamber design used in the present study, on a selected river
146 transect (~10 km) we have also tested the impact of the boat speed (5, 10, 20, 30 and 40 km h⁻¹) on the
147 sensor performance and have not detected any sizable (> 10%, p < 0.05, n = 25) difference in the CO₂
148 concentrations recorded by our system.

149 A Campbell logger was connected to the system allowing continuous recording of the CO₂
150 concentration (ppm), water temperature (°C) and pressure (mbar) every minute during 5 minutes over 10
151 minute intervals yielding 4,285 individual *p*CO₂, water temperature and pressure measurements in total.
152 These data were averaged for 3 consecutive slots of 5 min measurements, which represented the
153 approximate 20-km interval of the main stem route. CO₂ concentrations in the Lena River tributaries
154 were measured over the first 500-2000 m distance upstream of the tributary mouth, and comprised
155 between 5 and 34 measurements for day-time visits and between 305 and 323 individual *p*CO₂ readings
156 for each tributary for day-time and night-time monitoring.

157 Sensor preparation was conducted in the lab following the method described by Johnson et al.
158 (2009). The measurement unit (MI70, Vaisala®; accuracy ± 0.2%) was connected to the sensor allowing
159 instantaneous readings of *p*CO₂. The sensors were calibrated in the lab against standard gas mixtures (0,
160 800, 3 000, 8 000 ppm; linear regression with R² > 0.99) before and after the field campaign. The sensors'
161 drift was 0.03-0.06% per day and overall error was 4-8% (relative standard deviation, RSD). Following
162 calibration, post-measurement correction of the sensor output induced by changes in water temperature
163 and barometric pressure was done by applying empirically derived coefficients following Johnson et al.
164 (2009). These corrections never exceeded 5% of the measured values. Furthermore, we tested two
165 different sensors in several sites of the river transect: a main probe used for continuous measurements

166 and another probe used as a control and never employed for continuous measurements. We did not find
167 any sizable (>10%) difference in measured CO₂ concentration between these two probes.

168 For CH₄ analyses, unfiltered water was sampled in 60-mL Serum bottles and closed without air
169 bubbles using vinyl stoppers and aluminum caps and immediately poisoned by adding 0.2 mL of
170 saturated HgCl₂ via a two-way needle system. In the laboratory, a headspace was created by displacing
171 approx. 40% of water with N₂ (99.999%). Two 0.5-mL replicates of the equilibrated headspace were
172 analyzed for their concentrations of CH₄, using a Bruker GC-456 gas chromatograph (GC) equipped with
173 flame ionization and thermal conductivity detectors. After every 10 samples, a calibration of the detectors
174 was performed using Air Liquid gas standards (i.e. 145 ppmv). Duplicate injection of the samples showed
175 that results were reproducible within $\pm 5\%$. The specific gas solubility for CH₄ (Yamamoto et al., 1976)
176 was used in calculation of total CH₄ content in the vials and then recalculated to $\mu\text{mol L}^{-1}$ of the initial
177 waters.

178

179 *2.3. Chemical analyses of the river water*

180 The dissolved oxygen (CellOx 325; accuracy of $\pm 5\%$), specific conductivity (TetraCon 325;
181 $\pm 1.5\%$), and water temperature ($\pm 0.2\text{ }^{\circ}\text{C}$) were measured in-situ at 20 cm depth using a WTW 3320
182 Multimeter. The pH was measured using portable Hanna instrument via combined Schott glass electrode
183 calibrated with NIST buffer solutions (4.01, 6.86 and 9.18 at 25°C), with an uncertainty of 0.01 pH units.
184 The temperature of buffer solutions was within $\pm 5\text{ }^{\circ}\text{C}$ of that of the river water. The water was sampled
185 in pre-cleaned polypropylene bottle from 20-30 cm depth in the middle of the river and immediately
186 filtered through disposable single-use sterile Sartorius filter units (0.45 μm pore size). The first 50 mL of
187 filtrate was discarded. The DOC and Dissolved Inorganic Carbon (DIC) were determined by a Shimadzu
188 TOC-VSCN Analyzer (Kyoto, Japan) with an uncertainty of 3% and a detection limit of 0.1 mg/L. Blanks
189 of MilliQ water passed through the filters demonstrated negligible release of DOC from the filter
190 material.

191

192

193

2.4. Flux calculation

194 CO₂ flux (F_{CO_2}) was calculated following Cai and Wang (1998):

195
$$F_{CO_2} = K_h k_{CO_2} (C_{water} - C_{air}), \quad (1)$$

196 where K_h is the Henry's constant corrected for temperature and pressure (mol L⁻¹ atm⁻¹), k_{CO_2} is the gas
197 exchange velocity at a given temperature, C_{water} is the water CO₂ concentration, and C_{air} is the CO₂
198 concentration in the ambient air. In order to convert CO₂ concentration in water and air into CO₂ partial
199 pressure, we followed Wanninkhof et al. (1992) and Lauerwald et al. (2015). We used the average CO₂
200 concentrations of 402 ppm in May-June 2016 (from 129 stations all over the world,
201 <https://community.wmo.int/wmo-greenhouse-gas-bulletins>), which is consistent with the value recorded
202 at the nearest Tiksi station in 2016 (404±0.9 ppm, Ivakhov e al., 2019). Temperature-specific solubility
203 coefficients were used to calculate respective CO₂ concentrations in the water following Wanninkhof et
204 al. (1992). To standardize k_{CO_2} to a Schmidt number of 600, we used the following equation (Alin et al.,
205 2011; Vachon et al., 2010):

206
$$k_{600} = k_{CO_2} \left(\frac{600}{Sc_{CO_2}} \right)^{-n} \quad (2)$$

207 where Sc_{CO_2} is CO₂ Schmidt number for a given temperature (t , °C) in the freshwater (Wanninkhof, 1992):

208
$$Sc_{CO_2} = 1911.1 - 118.11t + 3.4527t^2 - 0.041320t^3 \quad (3)$$

209 The exponent n (Eqn. 2) is a coefficient that describes water surface (2/3 for a smooth water surface
210 regime while 1/2 for a rippled and a turbulent one), and the Schmidt number for 20°C in freshwater is
211 600. We used $n = 2/3$ because all water surfaces of sampled rivers were considered flat and had a laminar
212 flow (Alin et al., 2011; Jähne et al., 1987) with wind speed always below 3.7 m s⁻¹ (Guérin et al., 2007).

213 In this study, we used a k_{CO_2} (a median gas transfer coefficient) value of 4.464 m d⁻¹ measured in
214 the 4 largest rivers of Western Siberia Lowalnd (WSL) in June 2015 (Ob', Pur, Pyakupur and Taz rivers,
215 Karlsson et al., 2021). These rivers are similar to Lena and its tributaries in size, but exhibit lower velocity
216 than those of the Lena River. In fact, due to more mountainous relief, the Lena River main stem and
217 tributaries present much higher turbulence than that of the Ob River and tributaries and as such the value

218 k_{CO_2} used in this study can be considered rather conservative. This value is consistent with the k_{CO_2}
219 reported for the Kolyma River and its large tributaries ($3.9 \pm 2.5 \text{ m d}^{-1}$, Denfeld et al., 2013), tributaries
220 and main stem of the Yukon river basin ($4.9 - 7.6 \text{ m d}^{-1}$, Striegl et al. 2012), large rivers in the Amazon
221 and Mekong basins ($3.5 \pm 2.1 \text{ m d}^{-1}$, Alin et al., 2011) and with modelling results of k for large rivers
222 across the world ($3 - 4 \text{ m d}^{-1}$, Raymond et al., 2013). Note that decreasing the k to most conservative
223 value of 3 m d^{-1} of Raymond et al. (2013) will decrease specific emissions by ca. 30 %.

224 Instantaneous diffusive CH₄ fluxes were calculated using an equation similar to 1 with k from
225 western Siberia rivers (Serikova et al., 2018), concentrations of dissolved CH₄ in the water and air–water
226 equilibrium pCH₄ concentration of 1.8 ppm, and mean annual pCH₄ concentration in the air for 2016
227 (Mauna Loa Observatory ftp://aftp.cmdl.noaa.gov/products/trends/ch4/ch4_annmean_gl.txt) following
228 standard procedures (Serikova et al., 2018, 2019).

229

230 *2.5. Landscape parameters and water surface area of the Lena basin*

231 The physio-geographical characteristics of the 20 Lena tributaries sampled in this study and the
232 two points of the Lena main stem (upstream and downstream r. Aldan, **Table S1**) were determined by
233 applying available digital elevation model (DEM GMTED2010), soil, vegetation, lithological, and
234 geocryological maps. The landscape parameters were typified using TerraNorte Database of Land Cover
235 of Russia (Bartalev et al., 2020, <http://terranorte.iki.rssi.ru>). This included various type of forest
236 (evergreen, deciduous, needleleaf/broadleaf), grassland, tundra, wetlands, water bodies and other area.
237 The climate and permafrost parameters of the watershed were obtained from CRU grids data (1950-2016)
238 (Harris et al., 2014) and NCSCD data (<doi:10.5879/edds/00000001>, Hugelius et al., 2013), respectively,
239 whereas the biomass and soil OC content were obtained from BIOMASAR2 (Santoro et al., 2010) and
240 NCSCD databases. The lithology layer was taken from GIS version of Geological map of the Russian
241 Federation (scale 1 : 5 000 000, <http://www.geokarta.ru/>). To test the effect of carbonate rocks on
242 dissolved C parameters, we distinguished acidic crystalline, terrigenous silicate rocks and dolostones and
243 limestones of upper Proterozoic, Cambrian and Ordovician age. We quantified river water surface area
244 using the global SDG database with 30 m² resolution (Pekel et al., 2016) including both seasonal and

245 permanent water for the open water period of 2016 and for the multiannual average (reference period
246 2000-2004). We also used a more recent GRWL Mask Database which incorporates first order wetted
247 streams (Allen and Pavelsky, 2018).

248 The Pearson rank order correlation coefficient (Rs , $p < 0.05$) was used to determine the
249 relationship between CO_2 concentrations and climatic and landscape parameters of the Lena River
250 tributaries. Further statistical treatment of CO_2 , DIC and DOC concentration drivers in river waters
251 included a Principal Component Analysis which allowed to test the effect of various hydrochemical and
252 climatic parameters on dissolved C pattern. For the PCA treatment, all variables were normalized as
253 necessary in the standard package of STATISTICA-7 (<http://www.statsoft.com>) because the units of
254 measurement for various components were different. The factors were identified via the Raw Data
255 method. To run the scree test, we plotted the eigen values in descending order of their magnitude against
256 their factor numbers. There was significant decrease in the PCA values between F1 and F2 suggesting
257 that a maximum of two factors were interpretable.

258

259 **3. Results**

260 *3.1. CO_2 , CH_4 , DIC and DOC in the main stem and Lena tributaries and C emission fluxes*

261 The main hydrological C parameters of the Lena River and its tributaries (pCO_2 , CH_4 , pH, DIC,
262 and DOC) are listed in **Tables 1 and 2**. Continuous pCO_2 measurements in the main stem (4285
263 individual data points) averaged for each 20 km interval over the full distance of the boat route
264 demonstrated a sizable increase (from ca. 380 to 1040 μ atm) in pCO_2 northward (**Fig. 2**). There was a
265 positive correlation between the pCO_2 and distance from the head waters of the Lena River ($r = 0.625$, p
266 < 0.01 , **Fig. 3 A**). The CH_4 concentration was low (0.054 ± 0.023 and $0.061 \pm 0.028 \mu\text{mol L}^{-1}$ in the Lena
267 River and 20 tributaries, respectively) and did not change appreciably along the main stem and among
268 the 20 tributaries (**Fig. 3 B**). The DOC concentration did not demonstrate any systematic variations over
269 the main stem ($10.5 \pm 2.4 \text{ mg L}^{-1}$, **Fig. 3 C**), however it was higher and more variable in tributaries (15.8
270 $\pm 8.6 \text{ mg L}^{-1}$). The DIC concentration decreased about five-fold from the head waters to the middle course
271 of the Lena River (**Fig. 3 D**), and pH decreased by 0.8 units downstream (**Fig. 3 E**).

272 Generally, the concentrations of DOC measured in the present study during the peak of the spring
273 flood are at the highest range of previous assessments during summer baseflow (around 5 mg L⁻¹; range
274 of 2 to 12 mg L⁻¹, Cauwet and Sidorov, 1996; Lara et al., 1998; Lobbes et al., 2000; Kuzmin et al., 2009;
275 Kutscher et al., 2017). The DIC concentration in the main stem during spring flood was generally lower
276 than that reported during summer baseflow (around 10 mg L⁻¹; range of 5 to 50 mg L⁻¹) but consistent
277 with values reported in Yakutsk during May and June period (7 to 20 mg L⁻¹, Sun et al., 2018). A sizable
278 decrease in DIC concentration between the headwaters (first 500 km of the river) and the Lena River
279 middle course was also consistent with the alkalinity pattern reported in previous works during summer
280 baseflow (Pipko et al., 2010; Semiletov et al., 2011). For the Lena river tributaries, the most
281 comprehensive data set on major ions was acquired in July-August of 1991-1996 by Huh and Edmond's
282 group (Huh and Edmond, 1999; Huh et al., 1998a, b) and by Sun et al. (2018) in July 2012 and at the end
283 of June 2013. For most tributaries, the concentration of DIC was a factor of 2 to 5 lower during spring
284 flood compared to summer baseflow. This result can be explained by the strong dilution of carbonate-
285 rich groundwaters feeding the river in spring high flow compared to summer low flow.

286 The measured pCO₂ in the river water and published (Karlsson et al., 2021) gas transfer
287 coefficient (4.46 m d⁻¹) allowed for calculation of the CO₂ fluxes over the full length of the studied main
288 stem (2600 km) and the sampled tributaries. Calculated CO₂ fluxes of the main stem and tributaries
289 ranged from zero and slightly negative (uptake) values in the most southern part of the Lena River and
290 certain tributaries (N Katyma), to between 0.5-2.0 g C m⁻² d⁻¹ in the rest of the main stem and tributaries
291 (**Tables 1, 2; Fig. 2 B**). The largest part of the Lena River main stem, 1429 km from Kirenga to Tuolba,
292 exhibited quite stable flux of 1.1±0.2 g C m⁻² d⁻¹. In the last ~400 km part of the Lena River main stem
293 studied in this work, from Tuolba to Aldan, the calculated fluxes increased to 1.7±0.08 g C m⁻² d⁻¹.

294 The river water concentrations of dissolved CH₄ in the tributaries and the main channel
295 (0.059±0.006; IQR range from 0.025 to 0.199 μmol L⁻¹, **Table 1, 2**) did not exhibit any trend with
296 distance from headwaters or landscape parameters of the catchments. These values are consistent with
297 the range of CH₄ concentration in the low reaches of the Lena River main channel (0.03-0.085 μmol L⁻¹

298 ¹; Bussman, 2013) and are 100-500 times lower than those of CO₂. Consequently, diffuse CH₄ emissions
299 constituted less than 1 % of total C emissions and are not discussed in further detail.

300

301 *3.2. Diurnal (night/day) pCO₂ variations and spatial variations across the river transect*

302 The diel continuous CO₂ measurements of 3 tributaries (Kirenga, Tuolba and Aldan) and 14 sites
303 of the Lena River main channel showed generally modest variation with diurnal range within 10 % of
304 the average pCO₂ (**Fig. 4** and **Fig. S2**). The observed variations in pCO₂ between day and night were not
305 linked to water temperature ($p > 0.05$), which did not vary more than 1-2 °C between the day and night
306 period.

307 The spatial variations of hydrochemical parameters were tested in the upper reaches of the Lena
308 main stem and its largest tributary - the Aldan River (**Fig. S3**). In the Lena River, over a lateral distance
309 of 550 m across the river bed, the pCO₂ and CH₄ concentrations were equal to $569 \pm 4.6 \mu\text{atm}$ and
310 $0.0406 \pm 0.0074 \mu\text{mol L}^{-1}$, respectively, whereas the DIC and DOC concentrations varied $< 15\%$ ($n = 5$).
311 In the Aldan River, over a 2700 m transect across the flow, the pCO₂ and CH₄ concentrations were equal
312 to $1035 \pm 95 \mu\text{atm}$ and $0.078 \pm 0.00894 \mu\text{mol L}^{-1}$, respectively, whereas DIC and DOC varied within $< 20\%$
313 ($n = 4$). Overall, these results supported our design of punctual (snap shot) sampling in the middle of the
314 river.

315

316 *3.3. Impact of catchment characteristics on pCO₂ in tributaries of the Lena River*

317 The CO₂ concentration in the Lena River main stem and tributaries increased from southwest to
318 northeast (**Table 1, 2; Fig. 2**), and this was reflected in a positive ($R = 0.66$) correlation between CO₂
319 concentration and continuous permafrost coverage and a negative ($R = -0.76$) correlation with MAAT
320 (**Table 3**). Among different landscape factors, C stock in upper 0-30 and 0-100 cm of soil, the proportion
321 of riparian vegetation and bare rocks, the coverage by deciduous needle-leaf forest, and coverage of river
322 watershed by water bodies (mostly lakes) exhibited significant ($p < 0.01, n = 19$) positive correlations
323 ($0.54 \leq R \leq 0.86$) with average pCO₂ of the Lena River tributaries (**Fig. 5**). The other potentially important
324 landscape factors of the river watershed (proportion of peatland and bogs, tundra coverage, total

325 aboveground vegetation, type of permafrost, annual precipitation) did not significantly impact the CO₂
326 concentration in the Lena River tributaries (**Table 3**).

327 Further assessment of landscape factor control on C parameters of the river water was performed
328 via a PCA. This analysis basically confirmed the results of linear regressions and revealed two factors
329 capable explaining only 12.5 and 3.5% of variability (**Fig. S4**). The F1 strongly acted on the sample
330 location at the Lena transect, the content of OC in soils, the watershed coverage by deciduous needle-
331 leaf forest and shrubs, riparian vegetation (a proxy for the width of the riparian zone), but also proportion
332 of tundra, bare rock and soils, water bodies, peatland and bogs (> 0.90 loading). The pCO₂ was
333 significantly linked to F1 (0.72 loading).

334

335 *3.4. Areal emission from the Lena River basin*

336 The areal emission of CO₂ from the lotic waters of the Lena River watershed were assessed based
337 on total river water coverage of the Lena basin in 2016 (28,197 km², of which 5,022 km² is seasonal
338 water, according to the Global SDG database). This value is consistent with the total river surface area
339 from the GRWL Mask database (22,479 km²). Given that the measurements were performed at the peak
340 of spring flood in 2016, we used the maximal water coverage of the Lena River basin.

341 Based on past calculated pCO₂ of the Lena River (400 - 1000 μ atm, Semiletov, 1999; Semiletov
342 et al., 2011; Pipko et al., 2010) both the seasonality and spatial differences downstream are relatively
343 small. Indeed, for the lower reaches of the Lena River, from Yakutsk to the Lena Delta, Semiletov (1999)
344 and Semiletov et al. (2011) reported, for August-September 1995, the average pCO₂ of 538 \pm 96 μ atm
345 (range 380-727 μ atm). This value is very similar to the one obtained in July 2003 for the low reaches of
346 Lena (559 μ atm, Pipko et al., 2010). Over the full length of the Lena River, from Ust-Kut to the Lena
347 mouth, Pipko et al. (2010) reported an average pCO₂ of 450 \pm 100 μ atm in June-July 2003. At the same
348 time, calculated pCO₂ from previous field campaigns are generally lower than the pCO₂ of the Lena
349 River main stem directly measured in this study: 700-800 μ atm for the Ust Kut – Nuya segment (1331
350 km); 845 – 1050 μ atm for the Nuya – Aldan segment (1050 km).

351 Thus, despite the absolute values of calculated pCO₂ involving uncertainties (our calculated:
352 measured pCO₂ in Lena River main channel and tributaries equaled 0.67±0.15 (n = 47)), this suggests
353 spatial and temporal stability of the pCO₂ in the Lena River waters and allows for extrapolation of the
354 measured pCO₂ in the Lena River from Yakutsk to Aldan to the lower reaches of the river. As for the
355 Lena tributaries, to the best of our knowledge there is no published information on pCO₂ concentration
356 and emission. Overall, the major uncertainty in estimation of the Lena River basin emission stems from
357 a lack of direct pCO₂ measurements in the northern part of the main channel over ca. 1000 km
358 downstream of the Aldan River including the large tributary Vilyi. Further, we noted that the largest
359 northern tributary, the Aldan River providing 70% of the spring time discharge of the Lena River (Pipko
360 et al., 2010), demonstrated sizably higher emissions compared to the Lena River main channel upstream
361 of Aldan (3.2±0.5 and 1.69±0.08 g C m⁻² d⁻¹, respectively).

362 For areal emission calculations, we used the range of CO₂ emissions from 1 to 2 g C m⁻² d⁻¹ which
363 covers full variability of both large and small tributaries and the Lena River main channel (**Tables 1-2**,
364 **Figure 2 B**). This estimation assumes lack of pCO₂ dependence on the size of the watershed in the Lena
365 basin as confirmed by our data (**Fig. S5**). For an alternative areal emission calculations, we explicitly
366 took into account the water area of the main stem (43% relative to the total water area of the Lena
367 catchment) and we introduced the partial weight of emission from the 3 largest tributaries (Aldan,
368 Olekma and Vitim) according to their catchment surface areas (43, 12 and 14% of all sampled territory,
369 respectively). We summed up contribution of the Lena river main stem and the tributaries and we
370 postulated the average emission from the main stem upstream of Aldan (1.25±0.30 g C m⁻² d⁻¹) as
371 representative of the whole Lena River. This resulted in an updated value of 1.65±0.5 g C m⁻² d⁻¹ which
372 is within the range of 1 to 2 g C m⁻² d⁻¹ assessed previously. Note that this value is most likely
373 underestimated because emissions from the main stem downstream of Aldan are at least 10 % higher
374 (Table 1, Fig. 1 B).

375 For the two months of maximal water flow (middle of May - middle of July), the C emission from
376 the whole Lena basin equates to 2.8 ± 0.85 Tg C which is 20 to 30% of the DOC and DIC lateral export
377 to the Arctic Ocean. Assuming six months of open water period and no emission during winter, this

378 yields $8.3 \pm 2.5 \text{ Tg C y}^{-1}$ of annual emission for the whole Lena River basin ($2,490,000 \text{ km}^2$) with a total
379 lotic water area of $28,100 \text{ km}^2$. Considering the only $23,200 \text{ km}^2$ water area in July-October (and maximal
380 water coverage in May-June), these numbers decrease by 12% which is below the uncertainties
381 associated with our evaluation.

382

383

384 **4. DISCUSSION**

385 *4.1. Possible driving factors of CO₂ pattern in the Lena River basin*

386 Generally, the SW to NE increase in CO₂ concentrations and fluxes of the tributaries was
387 consistent with CO₂ pattern in the main stem (**Fig. 2**; **Tables 1, 2**), and thus can be considered as a
388 specific feature of CO₂ exchange between lotic waters and atmosphere in the studied part of the Lena
389 Basin. At the same time, there were sizable local variations (peaks) in CO₂ concentration of the main
390 stem along the sampling route (**Fig. 2 A**). Peaks shown on the diagram of the main stem are not
391 necessarily linked to CO₂-rich tributaries, but likely reflect local processes in the main stem, including
392 lateral influx from the shores and shallow subsurface waters, which is typical for permafrost regions of
393 forested Siberian watersheds (i.e., Bagard et al., 2011). Given that the data were averaged over $\sim 20\text{-km}$
394 distance, we believe that these peaks are not artifacts but reflect local heterogeneity of the pCO₂ pattern
395 in the main stem (turbulences, suprapermafrost water discharge, sediment resuspension and respiration).
396 Note that such a heterogeneity was not observed in the tributaries, at least at the scale of our spatial
397 coverage (see **Fig. S1 B, S3**).

398 The PCA demonstrated extremely low ability to describe the data variability (12% by F1 and only
399 3.5% by F2). We believe that the most likely reason of weak PCA capacity is the rather homogeneous
400 distribution of CO₂ and CH₄ among the tributaries, primarily linked to the specific hydrological period,
401 studied in this work - the spring flood. During this high flow period, the local lithological and soil
402 heterogeneities among tributaries or the segments of the main stem virtually disappear and surface flow
403 (via vegetation leaching) becomes the most important driver of riverine chemistry, as is known from

404 adjacent permafrost territories in Central Siberia (i.e., Bagard et al., 2011). Nevertheless, some specific
405 features of the data structure could be established. The first factor, significantly linked to pCO₂ (0.72
406 loading), strongly acted on the sample location at the Lena transect, the watershed coverage by deciduous
407 needle-leaf forest and shrubs, riparian vegetation, and also the proportion of tundra, bare rock and soils,
408 water bodies, peatland and bogs (> 0.90 loading). This is fully consistent with spatial variation of pCO₂
409 along the permafrost and climate gradient in the main channel and sampled tributaries. Positive loading
410 of riparian vegetation, peatlands and bogs on F1 (0.927 and 0.989, respectively) could reflect a
411 progressive increase in the feeding of the river basin by mire waters, an increase in the proportion of
412 needle-leaf deciduous trees, and in the width of the riparian zone from the SW to the NE direction.

413 Lack of sizable variation in pCO₂ between the day and night period or across the river bed
414 suggests quite low site-specific and diurnal variability. It may be indicative of a negligible role of primary
415 productivity in the water column given the low water temperatures, shallow photic layer of organic-rich
416 and turbid waters and lack of periphyton activity during high flow of the spring flood. The pCO₂
417 increased by a factor of 2 to 4 along the permafrost/temperature gradient from the southwest to the
418 northeast, for both the main channel and sampled tributaries. This may reflect progressive increase in the
419 feeding of the river basin by mire waters, increase in the proportion of needle-leaf deciduous forest, and
420 an increase in the width of the riparian zone. Another strong correlation is observed between the stock of
421 OC in soils (both 0-30 and 0-100 cm depth) and the pCO₂ of Lena tributaries. Organic-rich soils are
422 widely distributed in the central and northern part of the basin. The most southern part of the Lena basin
423 is dominated by carbonate rocks and crystalline silicates in generally mountainous terrain, where only
424 thin mineral soils are developed. The northern (downstream of the Olekma River) part of the basin
425 consists of soils developed on sedimentary silicate rocks as well as vast areas of easily eroded yedoma
426 soils. It is likely that both organic matter mineralization in OC-rich permafrost soils and lateral export of
427 CO₂ from these soils, together with particulate and dissolved OC export and mineralization in the water
428 column, are the main sources of CO₂ in the river water. Although some studies have demonstrated high
429 lability of DOM in arctic waters (Cory et al., 2014; Ward et al., 2017; Cory and Kling, 2018), others
430 suggest that DOM photo- and bio-degradation is low and does not support the major part of CO₂

431 supersaturation in water (Shirokova et al., 2019; Payandi-Rolland et al., 2020; Laurion et al., 2021). Note
432 that we have not observed any significant relationship between the DOC and pCO₂ in the Lena River and
433 tributaries (**Fig. S6 A**). Lack of such a correlation and absence of diurnal pCO₂ variations imply that in-
434 stream processing of dissolved terrestrial OC is not the main driver of CO₂ supersaturation in the river
435 waters of the Lena River basin. Furthermore, a lack of lateral (across the river bed) variations in pCO₂
436 does not support a sizable input of soil waters from the shore, although we admit that much higher spatial
437 coverage along the river shore is needed to confirm this hypothesis.

438 The role of underground water discharge in regulating pCO₂ pattern of the tributaries is expected
439 to be most pronounced in the SW part of the basin (Lena headwaters), where carbonate rocks of the
440 basement would provide sizable amounts of CO₂ discharge in the river bed. However, there was no
441 relationship between the proportion of carbonate rocks on the watershed and the pCO₂ in the tributaries
442 (**Fig. S6 B**). Furthermore, for the Lena River main stem, the lowest CO₂ concentrations were recorded in
443 the upper reaches (first 0-800 km) where carbonate rocks dominate. Altogether, this makes the impact of
444 CO₂ from underground carbonate reservoirs on river water CO₂ concentrations unlikely. This is further
445 illustrated by a lack of correlation between pCO₂ and DIC or pH (**Fig. S7 A** of the Supplement). The pH
446 did not control the CO₂ concentration in the main stem and only weakly impacted the CO₂ in the
447 tributaries (**Fig. S7 B**). The latter could reflect an increase in pCO₂ in the northern tributaries which
448 exhibited generally lower pH compared to the SW tributaries hosted within the carbonate rocks. Overall,
449 such low correlations of CO₂ with DIC and pH reflected a generally low predictive capacity to calculate
450 pCO₂ from measured pH, temperature and alkalinity (see section 3.4).

451 Therefore, other sources of riverine CO₂ may include particulate organic carbon processing in the
452 water column (Attermeyer et al., 2018), river sediments (Humborg et al., 2010) and within the riparian
453 zone (Leith et al., 2014, 2015) which require further investigation. In addition, although there was no
454 sizable variation in pCO₂ between the day and night period or across the river bed, the flux could show
455 different spatial and temporal patterns if *k* shows larger variability (cf., Beaulieu et al., 2012). This calls
456 for a need of direct flux measurements in representative rivers and streams of the Lena River basin.
457 Overall, the present study demonstrates highly dynamic and non-equilibrium behavior of CO₂ in the river

458 waters, with possible *hot spots* from various local sources. For these reasons, *in-situ*, high spatial
459 resolution measurements of CO₂ concentration in rivers—such as those reported for the Lena Basin in
460 this study—are crucially important for quantifying the C emission balance in lotic waters of high
461 latitudes.

462

463 *4.2. Areal emission from the Lena River basin vs lateral export to the Arctic Ocean*

464 The estimated CO₂ emissions from the Lena River main channel over 2600 km distance (0.8 –
465 1.7 g C m⁻² d⁻¹) are comparable to values directly measured in rivers and streams of the continuous
466 permafrost zone of western Siberia (0.98 g C m⁻² d⁻¹, Serikova et al., 2018), the Kolyma River (0.35 g C
467 m⁻² d⁻¹ in the main stem; 2.1 g C m⁻² d⁻¹ for lotic waters of the basin), and the Ob River main channel
468 (1.32±0.14 g C m⁻² d⁻¹ in the permafrost-free zone, Karlsson et al., 2021). At the same time, the Lena
469 River flux (FCO₂) values are lower than typical emissions from running waters in the contiguous Unites
470 States (3.1 g C m⁻² d⁻¹, Hotchkiss et al., 2015), small mountain streams in Northern Europe (3.3 g C m⁻²
471 d⁻¹, Rocher-Ros et al., 2019), and small streams of the northern Kolyma River (6 to 7 g C m⁻² d⁻¹, Denfeld
472 et al., 2013) and Ob River in the permafrost-affected zone (3.8 to 5.4 g C m⁻² d⁻¹, Karlsson et al., 2021).
473 In contrast to the main stem, the range of FCO₂ in the tributaries is larger (0.2 to 3.2 g C m⁻² d⁻¹) and
474 presumably reflects a strong variability in environmental conditions across a sizable landscape and
475 climate transect.

476 Total C emissions from other major Eastern Eurasian permafrost-draining rivers (i.e. sum of
477 Kolyma, Lena and Yenisei rivers) based on indirect estimates (40 Tg C y⁻¹, Raymond et al., 2013) are
478 generally supportive of the estimations of the Lena River in this study (5 to 10 Tg C y⁻¹). At the same
479 time, the C emission from the Lena river basin (28,100 km² water area) are lower than those of the lotic
480 waters of western Siberia (30 Tg C y⁻¹ for 33,389 km² water area, Karlsson et al., 2021). The latter drain
481 through thick, partially frozen peatlands within the discontinuous, sporadic and permafrost-free zones,
482 which can cause high OC input and processing and, thus, enhanced C emissions (Serikova et al., 2018).

483 Despite the high uncertainty on our regional estimations [due to lack of directly measured gas
484 transfer values and low seasonal resolution] we believe that these estimations are conservative and can

485 be considered as first order values pending further improvements. In order to justify extrapolation of our
486 data to all seasons and the entire area of the Lena basin, we analyzed data for spatial and temporal
487 variations in pCO₂ of the Lena River main stem from available literature. From the literature there were
488 three important findings. First, based on published data, the seasonal and spatial variabilities of pCO₂
489 across the majority of the Lena River main stem are not high during open water period, although the low
490 reaches of the Lena River may exhibit higher emissions compared to the middle and upper course (see
491 **section 3.4**). Second, although small mountainous headwater streams of the tributaries may exhibit high
492 k due to turbulence, this could be counteracted by lower CO₂ supply from low OC in mineral soil, lack
493 of riparian zone and scarce vegetation. Third, although these small streams (watershed area < 100 km²)
494 may represent > 60% of total watershed surfaces of the Lena basin (Ermolaev et al., 2018), their
495 contribution to the total water surface is < 20% (19% from combined analysis of DEM GMTED2010 and
496 16% from the GRWL or Global SDG database as estimated in this study). Therefore, given that (i) within
497 the stream-river continuum, the CO₂ efflux increases only two-fold demonstrating a discharge decrease
498 by a factor of 10,000 (from 100 to 0.01 m³ s⁻¹, Hotchkiss et al., 2015), and (ii) the watershed area had no
499 impact on pCO₂ in the river water (**Fig. S5**), this uncertainty is likely less important. As such, instead of
500 integrating indirect literature data, we used the pCO₂ values measured in the present study to calculate
501 the overall CO₂ emission from all lotic waters of the Lena basin.

502 The C evasion from the Lena basin assessed in the present work is comparable to the total
503 (DOC+DIC) lateral export by the Lena River to the Arctic Ocean (10 Tg C y⁻¹ by Semiletov et al. (2011),
504 or 11 Tg C y⁻¹ (5.35 Tg DIC y⁻¹ + 5.71 Tg DOC y⁻¹ by Cooper et al. (2008)). Moreover, the C evasion
505 strongly exceeds sedimentary C input to the Laptev Sea by all Siberian rivers (1.35 Tg C y⁻¹, Rachold et
506 al. (1996) and Dudarev et al. (2006)), the Lena River annual discharge of particulate organic carbon (0.38
507 Tg y⁻¹, Semiletov et al., 2011), and OC burial on the Kara Sea Shelf (0.37 Tg C y⁻¹, Gebhardt et al., 2005).

508 Typical concentrations of CH₄ in the Lena tributaries and the main channel are 100 to 500 times
509 lower than those of CO₂. Given that the global warming potential (GWP) of methane on a 100-year scale
510 is only 25 times higher than that of CO₂, the long-term role of diffuse methane emission from the Lena
511 River basin is still 4 to 20 times lower than that of CO₂. However, on a short-term scale (20 years), the

512 GWP of methane can be as high as 96 (Alvarez et al., 2018) and its role in climate regulation becomes
513 comparable to that of the CO₂. This has to be taken into account for climate modeling of the region.

514 The follow up studies of this large heterogenous and important system should include CO₂
515 measurements in 1) the low reaches of the Lena River, downstream of Aldan, notably large organic-rich
516 tributaries such as Vilyi (454,000 km²) and where the huge floodzone (20-30 km wide) with large number
517 of lakes and wetlands is developed, and 2) highly turbulent eastern tributaries of the Lena River
518 downstream of Aldan, which drain the Verkhoyansk Ridge and are likely to exhibit elevated gas transfer
519 coefficients.

520

521 **5. Conclusions**

522 Continuous pCO₂ measurements over 2600 km of the upper and middle part of the Lena River
523 main channel and 20 tributaries during the peak of spring flood allowed to quantify, for the first time, in-
524 situ pCO₂ variations which ranged from 500 to 1700 μatm and exhibited a 2 to 4-fold increase in CO₂
525 concentration northward. There was no major variation in pCO₂ between the day and night period or
526 across the river bed which supports the chosen sampling strategy. The northward increase in pCO₂ was
527 correlated with an increased proportion of needle-leaf deciduous trees, the width of the riparian zone and
528 the stock of organic C in soils. Among the potential drivers of riverine pCO₂, changes in the vegetation
529 pattern (northward migration of larch tree line in Siberia; Kruse et al., 2019) and soil OC stock are likely
530 to be most pronounced during ongoing climate warming and thus the established link deserves further
531 investigation. The total C emission from the lotic waters of the Lena River basin ranges from 5 to 10 Tg
532 C y⁻¹ which is comparable to the annual lateral export (50% DOC, 50 % DIC) by the Lena River to the
533 Arctic Ocean. However, these preliminary estimations of C emission should be improved by direct flux
534 measurements across seasons in different types of riverine systems of the basin, notably in the low
535 reaches of the Lena River.

536

537

538

539 **Acknowledgements.**
540 We acknowledge support from an RSF grant 18-17-00237_P, the Belmont Forum Project VULCAR-
541 FATE, and the Swedish Research Council (no. 2016-05275). We thank the Editor Ji-Hyung Park and 3
542 anonymous reviewers for their very constructive comments. Chris Benker is thanked for English
543 editing.

544

545 **Authors contribution.**
546 SV and OP designed the study and wrote the paper; SV, YK and OP performed sampling, analysis and
547 their interpretation; MK performed landscape characterization of the Lena River basin and calculated
548 water surface area; JK provided analyses of literature data, transfer coefficients for FCO₂ calculations
549 and global estimations of areal emission vs export.

550

551 **Competing interests.**

552 The authors declare that they have no conflict of interest.

553

554 **References**
555 Abril, G., Bouillon, S., Darchambeau, F., Teodoru, C. R., Marwick, T. R., Tamooh, F., Ochieng Omengo,
556 F., Geeraert, N., Deirmendjian, L., Polsenaere, P., and Borges, A. V.: Technical Note: Large
557 overestimation of pCO₂ calculated from pH and alkalinity in acidic, organic-rich freshwaters,
558 Biogeosciences, 12, 67–78, <https://doi.org/10.5194/bg-12-67-2015>, 2015.
559 Ahmed, R., Prowse, T., Dibike, Y., Bonsal, B., and O’Neil H.: Recent trends in freshwater influx to the
560 Arctic Ocean from four major Arctic-draining rivers, Water, 12, 1189; doi:10.3390/w12041189,
561 2020.
562 Alin, S. R., Rasera, M. F. F. L., Salimon, C. I., Richey, J. E., Holtgrieve, G. W., Krusche, A. V., et al. :
563 Physical controls on carbon dioxide transfer velocity and flux in low-gradient river systems and
564 implications for regional carbon budgets. J. Geophys. Res. Biogeosci. 116, G01009. doi:
565 10.1029/2010jg001398, 2011.
566 Allen, G. H. and Pavelsky, T. M.: Global extent of rivers and streams, Science 361, 585-58,
567 doi:10.1126/science.aat0636, 2018.
568 Alvarez, R. A., Zavala-Araiza, D., Lyon, D. R., Allen, D. T., Barkley, Z. R., Brandt, A. R., Davis, K.
569 J., Herndon, S. C., Jacob, D. J., Karion, A., Kort, E. A., Lamb, B. K., Lauvaux, T., Maasakkers, J.
570 J. D., Marchese, A. J., Omara, M., Pacala, S. W., Peischl, J., Robinson, A. L., Shepson, P. B., Sweeney,
571 C., Townsend-Small, A., Wofsy, S. C., Hamburg, S. P.: Assessment of methane emissions from the
572 U.S. oil and gas supply chain. Science 361, 186–188, doi:10.1126/science.aar7204, 2018.
573 Attermeyer, K., Catalan, N., Einarsdottir, K., Freixa, A., Groeneveld, M., Hawkes, J. A., et al.: Organic
574 carbon processing during transport through boreal inland waters: particles as important sites, J.
575 Geophys. Res. - Biogeosci. 123, 2412–2428, doi:10.1029/2018JG004500, 2018.
576 Bagard, M. L., Chabaux, F., Pokrovsky, O. S., Viers, J., Prokushkin, A. S., Stille, P., Rihs, S., Schmitt,
577 A. D., Dupre, B.: Seasonal variability of element fluxes in two Central Siberian rivers draining
578 high latitude permafrost dominated areas. Geochim. Cosmochim. Acta 75, 3335-3357, 2011.
579 Bartalev, S. A., Egorov, V. A., Ershov, D. V., Isaev, A. S., Lupyan, E. A., Plotnikov, D. E., and Uvarov,
580 I. A.: Remote mapping of vegetation land cover of Russia based on data of MODIS
581 spectroradimeter, Modern Problems of Earth Remote Sensing from Space, 8 (No 4), 285-302.
582 http://d33.infospace.ru/d33_conf/2011v8n4/285-302.pdf, 2011.

583 Beaulieu, J. J., Shuster, W. D., and Rebholz, J. A.: Controls on gas transfer velocities in a large river, *J.
584 Geophys. Res.*, 117, G02007, doi:10.1029/2011JG001794, 2012.

585 Berezovskaya, S., Yang, D., and Hinzman, L.: Long-term annual water balance analysis of the Lena
586 River, *Glob. Planet. Change* 48, 84–95, <https://doi.org/10.1016/j.gloplacha.2004.12.006>, 2005.

587 Brown, J., Ferrians Jr., O. J., Heginbottom, J. A., and Melnikov, E. S.: Circum-Arctic Map of Permafrost
588 and Ground Ice Conditions. National Snow and Ice Data Center/World Data Center for Glaciology,
589 Boulder, CO, USA, Digital media, 2002.

590 Bussmann I.: Distribution of methane in the Lena Delta and Buor-Khaya Bay, Russia, *Biogeosciences*
591 10, 4641-4652, <https://doi.org/10.5194/bg-10-4641-2013>, 2013.

592 Cai, W.-J. and Wang, Y.: The chemistry, fluxes, and sources of carbon dioxide in the estuarine waters of
593 the Satilla and Altamaha Rivers, Georgia, *Limnol. Oceanogr.* 43, 657–668.
594 <https://doi.org/10.4319/lo.1998.43.4.0657>, 1998.

595 Cauwet, G., and Sidorov I.: The biogeochemistry of Lena River: organic carbon and nutrients
596 distribution, *Marine Chem.* 53, 211-227, [https://doi.org/10.1016/0304-4203\(95\)00090-9](https://doi.org/10.1016/0304-4203(95)00090-9), 1996.

597 Chadburn, S. E., Krinner, G., Porada, P., Bartsch, A., Beer C. et al.: Carbon stocks and fluxes in the high
598 latitudes: using site-level data to evaluate Earth system models, *Biogeosciences* 14(22), 5143-5169,
599 <https://doi.org/10.5194/bg-14-5143-2017>, 2017.

600 Chevychelov, A. P., and Bosikov, N. P.: Natural Conditions, in: The Far North, edited by E.I. Troeva et
601 al., pp. 123, Springer, Netherlands, https://link.springer.com/chapter/10.1007/978-90-481-3774-9_1, 2010.

602 Cooper, L. W., McClelland, J. W., Holmes, R. M., Raymond, P. A., Gibson, J. J., Guay, C. K., and
603 Peterson, B. J.: Flow-weighted values of runoff tracers ($\delta^{18}\text{O}$, DOC, Ba, alkalinity) from the six
604 largest Arctic rivers, *Geophys. Res. Lett.*, 35, L18606, doi:10.1029/2008GL035007, 2008.

605 Cory, R. M., Ward, C. P., Crump, B. C., and Kling, G. W.: Sunlight controls water column processing
606 of carbon in arctic fresh waters, *Science*, 345, 925-928, doi: 10.1126/science.1253119, 2014.

607 Cory, R. M., Kling, G. W.: Interactions between sunlight and microorganisms influence dissolved
608 organic matter degradation along the aquatic continuum, *Limnol. Oceanogr. Lett.*, 3, 102–116,
609 <https://doi.org/10.1002/lol2.10060>, 2018.

610 Crawford, J. T., Loken, L. C., Casson, N. J., Smith, C., Stone, A. G, and Winslow, L. A.: High-speed
611 limnology: using advanced sensors to investigate spatial variability in biogeochemistry and
612 hydrology, *Environ. Sci. Technol.* 2015, 49, 1, 442–450, <https://doi.org/10.1021/es504773x>,
613 2015.

614 Denfeld, B.A., Frey K.E., Sobczak, W.V., Mann P.J., and Holmes, R.M.: Summer CO_2 evasion from
615 streams and rivers in the Kolyma River basin, north-east Siberia, *Polar Res.*, 32, Art No 19704,
616 <https://doi.org/10.3402/polar.v32i0.19704>, 2013.

617 Denfeld, B. A., Baulch, H. M., del Giorgio, P. A., Hampton, S. E., and Karlsson, J.: A synthesis of
618 carbon dioxide and methane dynamics during the ice-covered period of northern lakes,
619 *Limnology and Oceanography Letters* 3, 117-131, doi:10.1002/lol2.10079, 2018.

620 Dudarev, O. V., Semiletov, I. P., and Charkin, A. N.: Particulate material composition in the Lena River
621 - Laptev Sea system: Scales of heterogeneities, *Doklady Earth Sciences*, 411A (9), 1445-1451,
622 <https://link.springer.com/content/pdf/10.1134/S1028334X0609025X.pdf>, 2006.

623 Ermolaev, O. P., Maltzev K. A., Mukharamova S. S., Khomyakov P. V., and Shynbergenov E. A.:
624 Cartographic model of small rivers of the Lena River basin. *Ychenie Zapiski Kazansky Univ.,*
625 Ser. Natural Sciences, 160(1), 126-144, <https://cyberleninka.ru/article/n/kartograficheskaya-model-basseynovyh-geosistem-malyh-rek-vodosbora-reki-leny/viewer>, 2018.

626 Feng, X. J., Vonk, J. E., van Dongen, B. E., Gustafsson, O., Semiletov, I. P., Dudarev, O. V., Wang, Z.
627 H., Montlucon, D. B., Wacker, L., and Eglinton, T.I.: Differential mobilization of terrestrial carbon
628 pools in Eurasian Arctic river basins, *P. Natl. Acad. Sci. USA*, 110, 14168–14173,
629 <https://doi.org/10.1073/pnas.1307031110>, 2013.

630 Frey, K. E., and Smith, L.C.: Amplified carbon release from vast West Siberian peatlands by 2100,
631 *Geophys. Res. Lett.*, 32, L09401, doi:10.1029/2004GL022025, 2005.

632 Gautier, E., Depret, T., Costard, F., Virmoux, C., Fedorov, A. et al. : Going with the flow : Hydrologic
633 response of middle Lena River (Siberia) to the climate variability and change, *J. Hydrol.* 557, 475

636 - 488, <https://doi.org/10.1016/j.jhydrol.2017.12.034>, 2018.

637 Gebhardt, A. C., Gaye-Haake, B., Unger, D., Lahajnar, N., and Ittekkot, V.: A contemporary sediment
638 and organic carbon budget for the Kara Sea shelf (Siberia), *Marine Geology* 220(1-4), 83-100,
639 <https://doi.org/10.1016/j.margeo.2005.06.035>, 2005.

640 Gelfan, A., Gustafsson, D., Motovilov, Y., Arheimer, B., Kalugin, A., Krylenko, I., and Lavrenov A.:
641 Climate change impact on the water regime of two great Arctic rivers: modelling and uncertainty
642 issues, *Climate Change* 414(3), 499-515, DOI: 10.1007/s10584-016-1710-5m, 2017.

643 Georgiadi, A. G., Tananaev, N. I., and Dukhova L.A.: Hydrochemical conditions at the Lena River in
644 August 2018, *Oceanology* 59(5), 797-800, <https://doi.org/10.1134/S0001437019050072>, 2019.

645 Goncalves-Araujo, R., Stedmon, C. A., Heim, B., Dubinenkov, I., Kraberg, A., Moiseev, D., and Brachler
646 A.: From fresh to marine waters: Characterization and fate of dissolved organic matter in the Lena
647 River delta region, Siberia, *Front. Marine Sci.*, 2, Art No 108,
648 <https://doi.org/10.3389/fmars.2015.00108>, 2015.

649 Gordeev, V. V. and Sidorov, I. S.: Concentrations of major elements and their outflow into the Laptev
650 Sea by the Lena River, *Mar. Chem.*, 43, 33-46, 1993.

651 Griffin, C. G., McClelland, J. W., Frey, K. E., Fiske, G., and Holmes, R. M.: Quantifying CDOM and
652 DOC in major Arctic rivers during ice-free conditions using Landsat TM and ETM+ data. *Remote
653 Sens. Environ.* 209, 395-409, doi: 10.1016/j.rse.2018.02.060, 2018.

654 Guérin, F., Abril, G., Serça, D., Delon, C., Richard, S., Delmas, R., Tremblay, A., and Varfalvy, L.: Gas
655 transfer velocities of CO₂ and CH₄ in a tropical reservoir and its river downstream, *J. Mar. Syst.*,
656 66, 161-172. <https://doi.org/10.1016/j.jmarsys.2006.03.019>, 2007.

657 Gureyev, D.: Tomsk State University: The expedition on the Lena River from the headwaters to the
658 Aldan River, 2016. <https://www.youtube.com/watch?v=7IEiO4bgxc8>, 2016.

659 Harris, I., Jones, P. D., Osborn, T. J., and Lister, D. H.: Updated high-resolution grids of monthly climatic
660 observations – the CRU TS3.10 Dataset, *Int. J. Climatol.*, 34: 623-642, doi: 10.1002/joc.3711,
661 2014.

662 Hirst, K., Andersson, P., Kooijman, E., Kutscher, L., Maximov, T., Moth, C.-M., Porcelli, D.: Iron isotopes
663 reveal the sources of Fe-bearing particles and colloids in the Lena River basin, *Geochim. Cosmochim. Acta*, 269, 678-692, doi: 10.1016/j.gca.2019.11.004, 2020.

665 Holmes, R.M., Coe, M.T., Fiske, G.J., Gurtovaya, T., McClelland, J.W., Shiklomanov, A.I., Spencer,
666 R.G.M., Tank, S.E., and Zhulidov, A.V.: Climate change impacts on the hydrology and
667 biogeochemistry of Arctic Rivers, In: *Climatic Changes and Global warming of Inland Waters: Impacts and Mitigation for Ecosystems and Societies*, Eds. C.R. Goldman, M. Kumagi, and R.D.
668 Robarts, John Wiley and Sons, p. 1-26, 2013.

670 Horan, K.; Hilton, R. G., Dellinger, M., Tipper, E., Galy, V., Calmels, D., Selby, D., Gaillardet, J., Ottley,
671 C.J., Parsons, D.R., and Burton, K.W.: Carbon dioxide emissions by rock organic carbon oxidation
672 and the net geochemical carbon budget of the Mackenzie River Basin, *American J. Sci.* 319 (6) 473-
673 499, DOI: <https://doi.org/10.2475/06.2019.02>, 2019.

674 Hotchkiss, E., Hall Jr, R., Sponseller, R. et al.: Sources of and processes controlling CO₂ emissions change
675 with the size of streams and rivers, *Nature Geoscience*, 8, 696-699, <https://doi.org/10.1038/ngeo2507>,
676 2015.

677 Hugelius, G., Tarnocai, C., Broll, G., Canadell, J. G., Kuhry, P., and Swanson, D. K.: The Northern
678 Circumpolar Soil Carbon Database: spatially distributed datasets of soil coverage and soil carbon
679 storage in the northern permafrost regions, *Earth Syst. Sci. Data*, 5, 3-13, <https://doi.org/10.5194/essd-5-3-2013>, 2013.

681 Huh, Y., Tsoi, M. Y., Zaitsev, A., and Edmond, J. M.: The fluvial geochemistry of the rivers of eastern
682 Siberia: I. Tributaries of the Lena River draining the sedimentary platform of the Siberian Craton,
683 *Geochim. Cosmochim. Acta*, 62, 1657-1676, doi: 10.1016/S0016-7037(98)00107-0, 1998a.

684 Huh, Y., Pantelyev, G., Babich, O., Zaitsev, A., and Edmond, J. M.: The fluvial geochemistry of the rivers
685 of Eastern Siberia: II. Tributaries of the Lena, Omoloy, Yana, Indigirka, Kolyma, and Anadyr draining
686 the collisional/accretionary zone of the Verkhoyansk and Cherskiy ranges, *Geochim. Cosmochim.
687 Acta*, 62, 5063-5075, 1998b.

688 Huh, Y., and Edmond, J. M.: The fluvial geochemistry of the rivers of Eastern Siberia: III. Tributaries of the
689 Lena and Anabar draining the basement terrain of the Siberian Craton and the Trans-Baikal Highlands,
690 *Geochim. Cosmochim. Acta*, 63, 967–987, doi:10.1016/S0016-7037(99)00045-9, 1999.

691 Humborg, C., Morth, C.-M., Sundbom, M., Borg, H., Blenckner, T., Giesler, R., and Ittekkot, V.: CO₂
692 supersaturation along the aquatic conduit in Swedish watersheds as constrained by terrestrial
693 respiration, aquatic respiration and weathering, *Glob. Change Biol.*, 16, 1966–1978,
694 doi:10.1111/j.1365-2486.2009.02092.x, 2010.

695 Ivakhov, V. M., Paramonova, N. N., Privalov, V. I., Zinchenko, A. V., Loskutova, M. A., Makshtas, A.
696 P., Kustov, V. Y., Laurila, T., Aurela, M., and Asmi, E.: Atmospheric Concentration of Carbon
697 Dioxide at Tiksi and Cape Baranov Stations in 2010–2017, *Russian Meteorol. Hydrol.*, 44(4), 291–
698 299, DOI: 10.3103/S1068373919040095, 2019.

699 Jähne, B., Heinz, G., and Dietrich, W.: Measurement of the diffusion coefficients of sparingly soluble gases
700 in water, *J. Geophys. Res. Oceans* 92, 10767–10776, <https://doi.org/10.1029/JC092iC10p10767>,
701 1987.

702 Johnson, M. S., Billett, M. F., Dinsmore, K. J., Wallin, M., Dyson, K. E., and Jassal, R. S.: Direct and
703 continuous measurement of dissolved carbon dioxide in freshwater aquatic systems-method and
704 applications, *Ecohydrology* 3(1), 68–78, doi:10.1002/eco, 2009.

705 Juhls, B., Stedmon, C. A., Morgenstern, A., Meyer, H., Holemann, J., Heim, B., Povazhnyi, V., and
706 Overduin P. P.: Identifying drivers of seasonality in Lena River biogeochemistry and dissolved
707 organic matter fluxes, *Front. Environ. Sci.*, 8, Art No 53, <https://doi.org/10.3389/fenvs.2020.00053>,
708 2020.

709 Karlsson, J., Serikova, S., Rocher-Ros, G., Denfeld, B., Vorobyev, S. N., and Pokrovsky, O. S.: Carbon
710 emission from Western Siberian inland waters, *Nature Communication* 12, 825,
711 <https://doi.org/10.1038/s41467-021-21054-1>, 2021.

712 Klaus, M. and Vachon, D.: Challenges of predicting gas transfer velocity from wind measurements
713 over global lakes, *Aquatic Sciences* 82, Art No 53, doi:10.1007/s00027-020-00729-9, 2020.

714 Klaus, M., Seekell, D. A., Lidberg, W., and Karlsson, J.: Evaluations of climate and land management
715 effects on lake carbon cycling need to account temporal variability in CO₂ concentration,
716 *Global Biogeochemical Cycles*, 33, 243–265, doi:10.1029/2018gb005979, 2019.

717 Kruse, S., Gerdes, A., Kath, N. J., Epp, L. S., Stoof-Leichsenring, K. R., Pestryakova, L. A., and Herzschuh,
718 U.: Dispersal distances and migration rates at the arctic treeline in Siberia – a genetic and simulation-
719 based study, *Biogeosciences*, 16, 1211–1224, <https://doi.org/10.5194/bg-16-1211-2019>, 2019.

720 Kutscher, L., Mört, C.-M., Porcelli, D., Hirst, C., Maximov, T. C., Petrov, R. E., and Andersson, P. S.:
721 Spatial variation in concentration and sources of organic carbon in the Lena River, Siberia, *J. Geophys.
722 Res. Biogeosciences*, 122, 1999–2014, <https://doi.org/10.1002/2017JG003858>, 2017.

723 Kutzbach, L., Wille, C., and Pfeiffer, E.-M.: The exchange of carbon dioxide between wet arctic tundra and
724 the atmosphere at the Lena River Delta, Northern Siberia, *Biogeosciences* 4(5), 869–890,
725 <https://doi.org/10.5194/bg-4-869-2007>, 2007.

726 Kuzmin, M. I., Tarasova, E. N., Bychinskii, V. A., Karabanov, E. B., Mamontov, A. A., and Mamontova,
727 E. A.: Hydrochemical regime components of Lena water, *Water Resources* 36(4), 418–430,
728 <https://doi.org/10.1134/S0097807809040058>, 2009.

729 Lara, R. J., Rachold, V., Kattner, G., Hubberten, H. W., Guggenberger, G., Annelie, S., and Thomas, D. N.:
730 Dissolved organic matter and nutrients in the Lena River, Siberian Arctic: Characteristics and
731 distribution, *Marine Chemistry* 59, 301–309, doi: 10.1016/S0304-4203(97)00076-5, 1998.

732 Lauerwald, R., Laruelle, G. G., Hartmann, J., Ciais, P., Regnier, P. A. G.: Spatial patterns in CO₂ evasion
733 from the global river network, *Global Biogeochemical Cycles*, 29, 534–554.
734 <https://doi.org/10.1002/2014GB004941>, 2015.

735 Laurion, I., Massicotte, P., Mazoyer, F., Negandhi, K., and Mladenov, N.: Weak mineralization despite
736 strong processing of dissolved organic matter in Eastern Arctic tundra ponds, *Limnol. Oceanogr.*, 66,
737 (S1), S47–S63, doi: 10.1002/lno.11634, 2021.

738 Leith, F. I., Garnett, M. H., Dinsmore, K. J., Billett, M. F., and Heal, K. V.: Source and age of dissolved and
739 gaseous carbon in a peatland-riparian-stream continuum: a dual isotope (¹⁴C and $\delta^{13}\text{C}$) analysis,
740 *Biogeochemistry*, 119, 415–433, doi:10.1007/s10533-014-9977-y, 2014.

741 Leith, F. I., Dinsmore, K. J., Wallin, M. B., Billett, M; F., Heal, K. V., Laudon, H., Öquist, M. G., and
742 Bishop, K.: Carbon dioxide transport across the hillslope–riparian–stream continuum in a boreal
743 headwater catchment, *Biogeosciences*, 12, 1–12, doi:10.5194/bg-12-1-2015, 2015.

744 Lobbes, J. M., Friznar, H. P., and Kattner, G.: Biogeochemical characteristics of the dissolved and particulate
745 organic matter in Russian rivers entering the Arctic Ocean, *Geochim. Cosmochim. Acta*, 64(17),
746 2973–2983, 2000.

747 McClelland, J. W., Holmes, R. M., Peterson, B. J., and Strieglitz, M.: Increasing river discharge in the
748 Eurasian Arctic: Consideration of dams, permafrost thaw, and fires as potential agents of change, *J. Geophys. Res. Atmospheres*, 109 (D18), Art No D18102, doi:10.1029/2004JD004583, 2004.

750 McClelland, J. W., Déry, S. J., Peterson, B. J., Holmes, R. M., and Wood, E. F.: A pan-Arctic evaluation of
751 changes in river discharge during the latter half of the 20th century, *Geophys. Res. Lett.*, 33, L06715,
752 <https://doi.org/10.1029/2006GL025753>, 2006.

753 Murphy, M., Porcelli, D., Pogge von Strandmann, P., Hirst, K., Kutscher, L., Katchinoff, J., Morth, C.-
754 M., Maximov, T., and Andresson, P.: Tracing silicate weathering processes in the permafrost-
755 dominated Lena River watershed using lithium isotopes, *Geochim. Cosmochim. Acta*, 245, 154-
756 171, doi:10.1016/j.gca.2018.10.024, 2018.

757 Park, J. H., Jin, H., Yoon, T. K., Begum, M. S., Eliyan, C., Lee, E.-J., Lee, S.-C., and Oh, N.-H.:
758 Wastewater-boosted biodegradation amplifying seasonal variations of $p\text{CO}_2$ in the Mekong–Tonle
759 Sap river system, *Biogeochemistry*, 155, 219–235, <https://doi.org/10.1007/s10533-021-00823-6>,
760 2021.

761 Park, J.-H., Nayna, O.K., Begum, M.S., Chea, E., Hartmann, J., Keil, R.G., Kumar, S., Lu, X., Ran, L.,
762 Richey, J.E., Sarma, V.V.S.S., Tareq, S.M., Xuan, D. T., and Yu, R.: Reviews and syntheses:
763 Anthropogenic perturbations to carbon fluxes in Asian river systems—concepts, emerging trends,
764 and research challenges, *Biogeosciences* 15, 3049–3069. <https://doi.org/10.5194/bg-15-3049-2018>, 2018.

765 Payandi-Rolland, D., Shirokova, L. S., Nakhle, P., Tesfa, M., Abdou, A., Causserand, C., Lartiges, B.,
766 Rols, J.L., Guérin, F., Bénézeth, P., and Pokrovsky, O.S.: Aerobic release and biodegradation of
767 dissolved organic matter from frozen peat: Effects of temperature and heterotrophic bacteria,
768 *Chem. Geol.* 536, Art No 119448, <https://doi.org/10.1016/j.chemgeo.2019.119448>, 2020.

770 Pekel, J. F., Cottam, A., Gorelick, N. et al.: High-resolution mapping of global surface water and its long-
771 term changes, *Nature*, 540, 418–422, <https://doi.org/10.1038/nature20584>, 2016.

772 Pipko, I. I., Pugach, S. P., Savichev, O. G., Repina, I. A., Shakhova, N. E., Moiseeva, Yu. A., Barskov, K.
773 V., Sergienko, V. I., and Semiletov, I. P.: Dynamics of dissolved inorganic carbon and CO₂ fluxes
774 between the water and the atmosphere in the main channel of the Ob River, *Doklady Chemistry*
775 484(2), 52-57, doi:10.1134/S0012500819020101, 2019.

776 Pipko; I. I., Pugach, S. P., Dudarev, O. V., Charkin, A. N., and Semiletov, I. P.: Carbonate parameters
777 of the Lena River: Characteristics and distribution, *Geochem. Internat.*, 48(11), 1131-1137,
778 <https://doi.org/10.1134/S0016702910110078>, 2010.

779 Qin, J., Huh, Y., Edmond, J. M., Du, G., and Ran, J.: Chemical and physical weathering in the Min
780 Jiang, a headwater tributary of the Yangtze River, *Chem. Geol.*, 227, 53–69,
781 doi:10.1016/j.chemgeo.2005.09.011, 2006.

782 Rachold, V., Alabyan, A., Hubberten, H.-W., Korotaev, V. N., and Zaitsev, A. A.: Sediment transport
783 to the Laptev Sea - hydrology and geochemistry of the Lena River, *Polar Research*, 15(2), 183-
784 196, doi: <https://doi.org/10.3402/polar.v15i2.6646>, 1996.

785 Raymond, P. A., McClelland, J. W., Holmes, R. M., Zhulidov, A. V., Mull, K. et al.: Flux and age of
786 dissolved organic carbon exported to the Arctic Ocean: A carbon isotopic study of the five
787 largest arctic rivers, *Global Biogeochemical Cycles*, 121, Art No GB4011,
788 <https://doi.org/10.1029/2007GB002934>, 2007.

789 Raymond, P. A., Hartmann, J., Lauerwald, R., Sobek, S., McDonald, C., Hoover, M., Butman, D., Striegl,
790 R., Mayorga, E., Humborg, C., Kortelainen, P., Dürr, H., Meybeck, M., Ciais, P., and Guth, P.:
791 Global carbon dioxide emissions from inland waters, *Nature*, 503, 355–359,
792 doi:10.1038/nature12760, 2013.

793 Rocher-Ros, G., Sponseller, R. A., Lidberg, W., Mörth, C-M., and Giesler, R.: Landscape process
794 domains drive patterns of CO₂ evasion from river networks, *Limnol. Oceanogr. Lett.*, 4, 87-95,
795 <https://doi.org/10.1002/10l2.10108>, 2019.

796 Sachs, T., Wille, C., Boike, J., and Kutzbach, L.: Environmental controls on ecosystem-scale CH₄ emission
797 from polygonal tundra in the Lena River Delta, Siberia, *J. Geophys. Research Biogeosciences*, 113,
798 Art No G00A03, <https://doi.org/10.1029/2007JG000505>, 2008.

799 Santoro, M., Beer, C., Cartus, O., Schmullius, C., Shvidenko, A., McCallum, I., Wegmueller, U., and
800 Wiesmann, A.: The BIOMASAR algorithm: An approach for retrieval of forest growing stock volume
801 using stacks of multi-temporal SAR data, In: Proceedings of ESA Living Planet Symposium, 28 June-
802 2 July 2010 (<https://www.researchgate.net/publication/230662433>,
803 <http://pure.iiasa.ac.at/id/eprint/9430/>, 2010.

804 Schuur, E. A. G., McGuire, A. D., Schädel, C., Grosse, G., Harden, J. W., Hayes, D. J., Hugelius, G., Koven,
805 C. D., Kuhry, P., Lawrence, D. M., Natali, S. M., Olefeldt, C., Romanovsky, V. E., Schaefer, K.,
806 Turetsky, M. R., Treat, C. C., and Vonk, J. E.: Climate change and the permafrost carbon feedback,
807 *Nature* 520, 171-179, <http://dx.doi.org/10.1038/nature14338>, 2015.

808 Semiletov, I. P.: Aquatic sources and sinks of CO₂ and CH₄ in the polar regions, *J. Atmospheric Sci.*, 56,
809 286-306, [https://doi.org/10.1175/1520-0469\(1999\)056<0286:ASASOC>2.0.CO;2](https://doi.org/10.1175/1520-0469(1999)056<0286:ASASOC>2.0.CO;2), 1999.

810 Semiletov, I. P., Pipko, I. I., Shakhova, N. E., Dudarev, O. V., Pugach, S. P., Charkin, A. N., McRoy, C. P.,
811 Kosmach, D., Gustafsson Ö.: Carbon transport by the Lena River from its headwaters to the Arctic
812 Ocean, with emphasis on fluvial input of terrestrial particulate organic carbon vs. carbon transport by
813 coastal erosion, *Biogeosciences*, 8, 2407-2426, <https://doi.org/10.5194/bg-8-2407-2011>, 2011.

814 Serikova, S., Pokrovsky, O. S., Ala-aho, P., Kazantsev, V., Kirpotin, S. N., Kopysov, S. G., Krickov, I. V.,
815 Laudon, H., Manasypov, R. M., Shirokova, L. S., Sousby, C., Tetzlaff, D., and Karlsson, J.: High
816 riverine CO₂ emissions at the permafrost boundary of Western Siberia, *Nat. Geosci.*, 11, 825-829,
817 <https://doi.org/10.1038/s41561-018-0218-1>, 2018.

818 Serikova S., Pokrovsky O. S., Laudon, H., Krickov, I. V., Lim, A. G., Manasypov, R. M., and Karlsson, J.:
819 C emissions from lakes across permafrost gradient of Western Siberia, *Nat. Commun.*, 10, 1552,
820 <https://doi.org/10.1038/s41467-019-09592-1>, 2019.

821 Siewert, M. B., Hugelius, G., Heim, B., and Faucherre, S.: Landscape controls and vertical variability of soil
822 organic carbon storage in permafrost-affected soils of the Lena River Delta, *Catena*, 147, 725-741,
823 doi:10.1016/j.catena.2016.07.048, 2016.

824 Smith, L. C., Pavelksky, T. M.: Estimation of river discharge, propagation speed, and hydraulic
825 geometry from space: Lena River, Siberia, *Water Resources Res.*, 44(3), W03427,
826 <https://doi.org/10.1029/2007WR006133>, 2008.

827 Spence, J. and Telmer, K.: The role of sulfur in chemical weathering and atmospheric CO₂ fluxes:
828 evidence from major ions, $\delta^{13}\text{CDIC}$, and $\delta^{34}\text{SSO}_4$ in rivers of the Canadian Cordillera, *Geochim.
829 Cosmochim. Acta*, 69, 5441-5458, doi:10.1016/j.gca.2005.07.011, 2005.

830 Stackpoole, S. M., Butman, D. E., Clow, D. W., Verdin, K. L., Gaglioti, B. V., Genet, H., and Striegl,
831 R. G.: Inland waters and their role in the carbon cycle of Alaska, *Ecological Applications* 27(5),
832 1403-1420, doi:10.1002/ea.1552/full, 2017.

833 Striegl, R. G., Dornblaser, M. M., McDonald, C. P., Rover, J. R., and Stets E. G.: Carbon dioxide and
834 methane emissions from the Yukon River system, *Global Biogeochem. Cycles*, 26, GB0E05,
835 doi:10.1029/2012GB004306, 2012.

836 Sun X., Mörth C.-M., Porcelli D., Kutscher L., Hirst C., Murphy M. J., Maximov T., Petrov R. E.,
837 Humborg C., Schmitt M. and Andersson P. S.: Stable silicon isotopic compositions of the Lena
838 River and its tributaries: Implications for silicon delivery to the Arctic Ocean, *Geochim.
839 Cosmochim. Acta* 241, 120-133, doi: 10.1016/j.gca.2018.08.044, 2018.

840 Suzuki, K., Matsuo, K., Yamazaki, D., Ichii, K., Iijima, Y., Papa, F., Yanagi, Y., and Hiyama, T.:
841 Hydrological variability and changes in the Arctic circumpolar tundra and the three largest Pan-
842 Arctic river basins from 2002 to 2016, *Remote Sensing* 10, Art No 402, doi:10.3390/rs10030402,
843 2018.

844 Vachon, D., Prairie, Y. T., and Cole, J. J.: The relationship between near-surface turbulence and gas
845 transfer velocity in freshwater systems and its implications for floating chamber measurements of

846 gas exchange, Limnology and Oceanography, 55(4), 1723–173, doi:10.4319/lo.2010.55.4.1723,
847 2010.

848 Van der Molen, M. K., van Huissteden J., Parmentier F. J. W., Petrescu, A. M. R., Dolman, A. J.,
849 Maximov, T. C. et al.: The growing season greenhouse gas balance of a continental tundra site in
850 the Indigirka lowlands, NE Siberia, Biogeosciences 4(6), 985-1003, <https://doi.org/10.5194/bg-4-985-2007>, 2007.

852 Vonk, J. E., Tank, S. E., Mann, P. J., Spencer, R. G. M., Treat, C. C., Striegl, R. G., Abbott, B. W., and
853 Wickland, K. P.: Biodegradability of dissolved organic carbon in permafrost soils and aquatic
854 systems: a meta-analysis, Biogeosciences, 12, 6915–6930, <https://doi.org/10.5194/bg-12-6915-2015>, 2015.

856 Vonk, J. E., Tank, S. E., and Walvoord, M. A.: Integrating hydrology and biogeochemistry across frozen
857 landscapes, Nat. Commun. 10, 1–4. <https://doi.org/10.1038/s41467-019-13361-5>, 2019.

858 Wanninkhof, R.: Relationship between wind speed and gas exchange over the ocean, J. Geophys. Res.
859 97, 7373–7382, <https://doi.org/10.4319/lom.2014.12.351>, 1992.

860 Ward, C. P., Nalven, S. G., Crump, B. C., Kling, G. W., and Cory, R. M.: Photochemical alteration of
861 organic carbon draining permafrost soils shifts microbial metabolic pathways and stimulates
862 respiration, Nat. Commun., 8, 772, <https://doi.org/10.1038/s41467-017-00759-2>, 2017.

863 Wild, B., Andersson, A., Bröder, L., Vonk, J., Hugelius, G., McClelland, J. W., Song, W., Raymond P.
864 A., and Gustafsson, Ö.: Rivers across the Siberian Arctic unearth the patterns of carbon release
865 from the thawing permafrost, PNAS 116(21), 10280-10285,
866 <https://doi.org/10.1073/pnas.1811797116>, 2019.

867 Wille, C., Kutzbach, L., Sachs, T., Wagner, D., and Pfeiffer, E.M.: Methane emission from Siberian
868 arctic polygonal tundra: eddy covariance measurements and modeling, Global Change Biology
869 14(6), 1395-1408, <https://doi.org/10.1111/j.1365-2486.2008.01586.x>, 2008.

870 Wu, L. and Huh, Y.: Dissolved reactive phosphorus in large rivers of East Asia, Biogeochemistry 85,
871 263-288, doi:10.1007/s10533-007-9133-z, 2007.

872 Yang, D. Q., Kane, D. L., Hinzman, L. D., Zhang, X. B., Zhing, T. J., and Ye, H. C.: Siberian Lena River
873 hydrological regime and recent change, J. Geophys. Res. Atmopsheres 107, D23, Art No 4694,
874 <https://doi.org/10.1029/2002JD002542>, 2002.

875 Yamamoto, S., Alcauskas, J. B., and Crozier, T.E.: Solubility of methane in distilled water and seawater,
876 J. Chem. Eng. Data, 21(1), 78– 80, doi:10.1021/je60068a029, 1976.

877 Ye, B., Yang, D., Zhang, Z., and Kane, D. L.: Variation of hydrological regime with permafrost coverage
878 over Lena basin in Siberia, J. Geophys. Res., 114, D07102, doi:10.1029/2008JD010537, 2009.

879 Yoon, T. K., Jin, H., Oh, N.-H., and Park, J.-H.: Technical note: Assessing gas equilibration systems for
880 continuous pCO₂ measurements in inland waters, Biogeosciences, 13, 3915–3930,
881 <https://doi.org/10.5194/bg-13-3915-2016>, 2016.

882 Zhang, T., Frauenfeld, O. W., Serreze, M. C., Etringer, A., Oelke, C. et al.: Spatial and temporal
883 variability in active layer thickness over the Russian Arctic drainage basin, J. Geophys. Res., 110,
884 D16101, doi: 10.1029/2004JD005642, 2005.

885 Zubrzycki, S., Kutzbach, L., Grosse, G., Desyatkin, A., and Pfeiffer, E. M.: Organic carbon and total
886 nitrogen stocks in soils of the Lena River Delta, Biogeosciences 10, 3507-3524, doi:10.5194/bg-
887 10-3507-2013, 2013.

888

889

890

891

892

893

894

895 **Table 1.** Measured water temperature, pCO₂, calculated CO₂ flux, CH₄, DOC, and DIC concentrations
 896 and pH in the Lena River main stem (average \pm s.d.; (n) is number of measurements).

897

River transect	T _{water} , °C	pCO ₂ , μatm	FCO ₂ , g C m ⁻² d ⁻¹ <i>k</i> = 4.464
Lena upstream of Kirenga (0-578 km)	12.65 \pm 0.22 (99)	714 \pm 22 (99)	0.849 \pm 0.061 (99)
Lena Kirenga – Vitim (579-1132 km)	9.17 \pm 0.15 (87)	806 \pm 8.8 (87)	1.19 \pm 0.024 (87)
Lena Vitim -Nuya (1132-1331 km)	8.10 \pm 0.115 (27)	797 \pm 22 (27)	1.22 \pm 0.072 (27)
Lena Nuya – Tuolba (1331-2008 km)	9.61 \pm 0.09 (95)	846 \pm 12 (95)	1.29 \pm 0.034 (95)
Lena Tuolba – Aldan (2008-2381 km)	10.6 \pm 0.21 (52)	1003 \pm 28 (52)	1.69 \pm 0.081 (5)

898

	CH ₄ , $\mu\text{mol L}^{-1}$	DOC, mg L ⁻¹	DIC, mg L ⁻¹	pH
Lena upstream of Kirenga (0-578 km)	0.068 \pm 0.003 (6)	13.9 \pm 1.4 (6)	20.0 \pm 1.2 (6)	8.12 \pm 0.203 (7)
Lena Kirenga – Vitim (579-1132 km)	0.040 \pm 0.002 (12)	7.55 \pm 0.246 (14)	6.30 \pm 0.485 (14)	7.77 \pm 0.040 (14)
Lena Vitim -Nuya (1132-1331 km)	0.038 \pm 0.003 (5)	9.02 \pm 0.29 (3)	4.55 \pm 0.70 (3)	7.69 \pm 0.063 (3)
Lena Nuya – Tuolba (1331-2008 km)	0.037 \pm 0.002 (6)	10.4 \pm 0.78 (2)	5.09 \pm 1.157 (2)	7.62 \pm 0.052 (2)
Lena Tuolba – Aldan (2008-2381 km)	0.088 \pm 0.034 (5)	11.6 \pm 0.27 (5)	5.24 \pm 0.102 (5)	7.49 \pm 0.044 (5)

899

900

901

902

903

904

905

906

907

908

909

910

911

912

913

914

915

916

917

918

919

920

921

922 **Table 2.** Measured water temperature, pCO₂, calculated CO₂ flux, CH₄, DOC, DIC concentration and
 923 pH in the tributaries (average \pm s.d.; (n) is number of measurements).

924

Tributary	T _{water} , °C	pCO ₂ , μatm	FCO ₂ , g C m ⁻² d ⁻¹
№4 Orlinga (208 km)	8.0 \pm 0.0 (13)	515 \pm 2.9 (13)	0.347 \pm 0.01 (13)
№5 Nijnaya Kitima (228 km)	6.8 \pm 0.0 (11)	462 \pm 9.4 (11)	0.193 \pm 0.03 (11)
№8 Taiur (416 km)	8.5 \pm 0.0 (10)	575 \pm 31 (10)	0.523 \pm 0.095 (10)
№10 Bol. Tira (529 km)	11.9 \pm 0.0 (15)	788 \pm 12 (15)	1.04 \pm 0.03 (15)
№12 Kirenga (579 km)	10.2 \pm 0.0 (323)	448 \pm 4 (323)	0.131 \pm 0.01 (323)
№25 Thcayka (1025 km)	8.6 \pm 0.01 (8)	856 \pm 13 (8)	1.37 \pm 0.04 (8)
№28 Tchuya (1110 km)	5.9 \pm 0.0 (5)	751 \pm 5.7 (5)	1.16 \pm 0.019 (5)
№29 Vitim (1132 km)	6.8 \pm 0.0 (10)	654 \pm 10 (10)	0.812 \pm 0.03 (10)
№32 Ykte (1265 km)	4.9 \pm 0.0 (11)	676 \pm 4.8 (11)	0.943 \pm 0.02 (11)
№34 Kenek (1312 km)	7.60 \pm 0.0 (11)	710 \pm 2.6 (11)	0.964 \pm 0.01 (11)
№36 Nuya (1331 km)	11.8 \pm 0.0 (10)	752 \pm 6.0 (10)	0.947 \pm 0.02 (10)
№38 Bol. Patom (1670 km)	6.9 \pm 0.0 (5)	730 \pm 12 (5)	1.05 \pm 0.04 (5)
№39 Biriuk (1712 km)	14.2 \pm 0.0 (5)	929 \pm 19 (5)	1.32 \pm 0.05 (5)
№40 Olekma (1750 km)	6.4 \pm 0.0 (11)	802 \pm 14 (11)	1.30 \pm 0.05 (11)
№43 Markha (1948 km)	17.5 \pm 0.0 (15)	844 \pm 15 (15)	0.998 \pm 0.03 (15)
№44 Tuolba (2008 km)	12.3 \pm 0.0 (305)	1181 \pm 6 (305)	2.08 \pm 0.02 (305)
№46 Siniaya (2118 km)	18.5 \pm 0.0 (24)	894 \pm 19 (24)	1.08 \pm 0.04 (24)
№48 Buotama (2170 km)	18.5 \pm 0.0 (24)	1160 \pm 25 (24)	1.66 \pm 0.06 (24)
№52-54 Aldan (2381 km)	14.8 \pm 0.02 (316)	1715 \pm 12 (316)	3.23 \pm 0.03 (316)

925

926

927

928

929

930

931

932

933

934

935

936

937

938

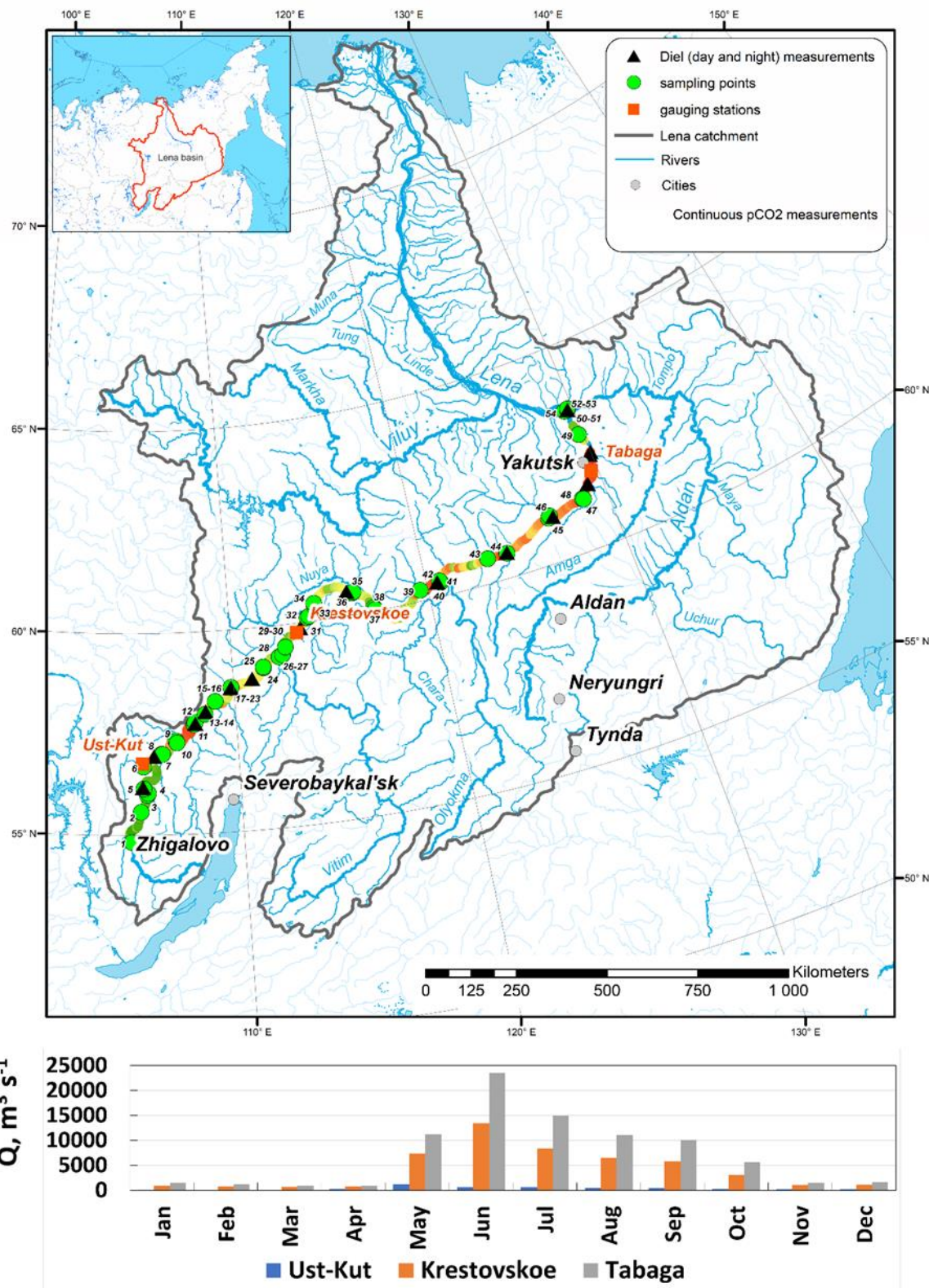
Table 2, continued.

	CH ₄ , μmol L ⁻¹	DOC, mg L ⁻¹	DIC, mg L ⁻¹	pH
№4 Orlinga (208 km)	0.064	13.4	27.9	8.64
№5 Nijnaya Kitima (228 km)	0.033	16.7	13.1	8.48
№8 Taiur (416 km)	0.079	10.0	11.2	8.36
№10 Bol. Tira (529 km)	0.084	22.7	14.9	8.13
№12 Kirenga (579 km)	0.036	5.13	6.86	7.97
№25 Thcayka (1025 km)	0.066	16.7	22.5	8.30
№28 Tchuya (1110 km)	0.037	7.08	3.44	7.57
№29 Vitim (1132 km)	0.057	10.1	2.18	7.70
№32 Ykte (1265 km)	0.037	5.49	15.3	7.86
№34 Kenek (1312 km)	0.053	21.1	16.0	8.12
№36 Nuya (1331 km)	0.048	26.6	11.7	7.80
№38 Bol. Patom (1670 km)	0.026	6.99	4.56	7.76
№39 Biriuk (1712 km)	0.047	29.2	11.3	7.87
№40 Olekma (1750 km)	0.046	13.3	3.3	7.53
№43 Markha (1948 km)	0.088	27.4	10.9	8.00
№44 Tuolba (2008 km)	0.035	14.5	14.7	7.98
№46 Siniaya (2118 km)	0.113	33.2	7.73	7.97
№48 Buotama (2170 km)	0.124	12.2	31.6	8.45
№52-54 Aldan (2381 km)	0.088 (4)	9.07±0.75 (4)	6.67±0.13 (4)	7.59±0.02 (4)

Footnote : in all tributaries except Aldan, there was only one measurement of CH₄, DOC, DIC and pH

944 **Table 3.** Pearson correlation coefficients (**R**) between pCO₂ and landscape parameters of the Lena
 945 tributaries. Significant correlations ($p < 0.05$) are marked by asterisk. Methane concentration did not
 946 exhibit any significant correlation with all tested parameters.

% coverage of the watershed and climate	R 948
Broadleaf Forest	0.04
Humid Grassland	-0.52*
Shrub Tundra	-0.05
Riparian Vegetation	0.87*
Croplands	-0.31
Bare Soil and Rock	0.54*
Evergreen Needle-leaf Forest	-0.59*
Deciduous Broadleaf Forest	-0.14
Mixed Forest	-0.34
Deciduous Needle-leaf Forest	0.56*
Bogs and marches	0.44
Palsa bogs	0.29
Recent burns	-0.25
Water bodies	0.63*
Aboveground biomass	-0.55*
Soil C stock, 0-30 cm	0.54*
Soil C stock, 0-100 cm	0.65*
Carbonate rocks	0.20
Continuous permafrost	0.66*
Discontinuous permafrost	-0.27
Sporadic permafrost	-0.43
Isolated permafrost	-0.19
Mean annual air temperature	-0.76*
Mean annual precipitation, mm	0.10



951

952 **Fig. 1.** Map of the studied Lena River watershed with continuous pCO₂ measurements in the main
 953 stem. Bottom: mean multi-annual monthly discharge (Q) at Ust-Kut, Krestovskoe and Tabaga station
 954 (labelled in red on the map).

955

956

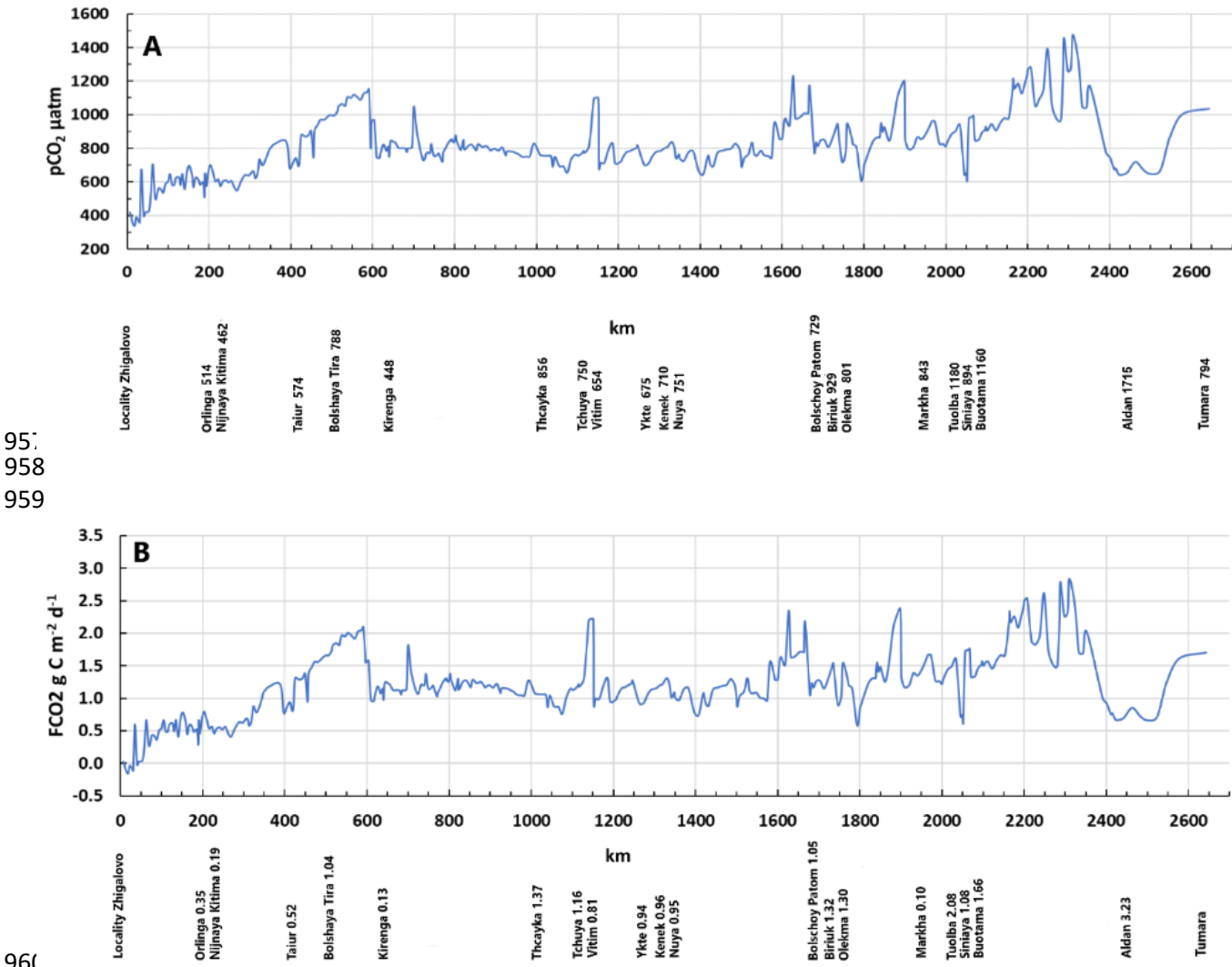
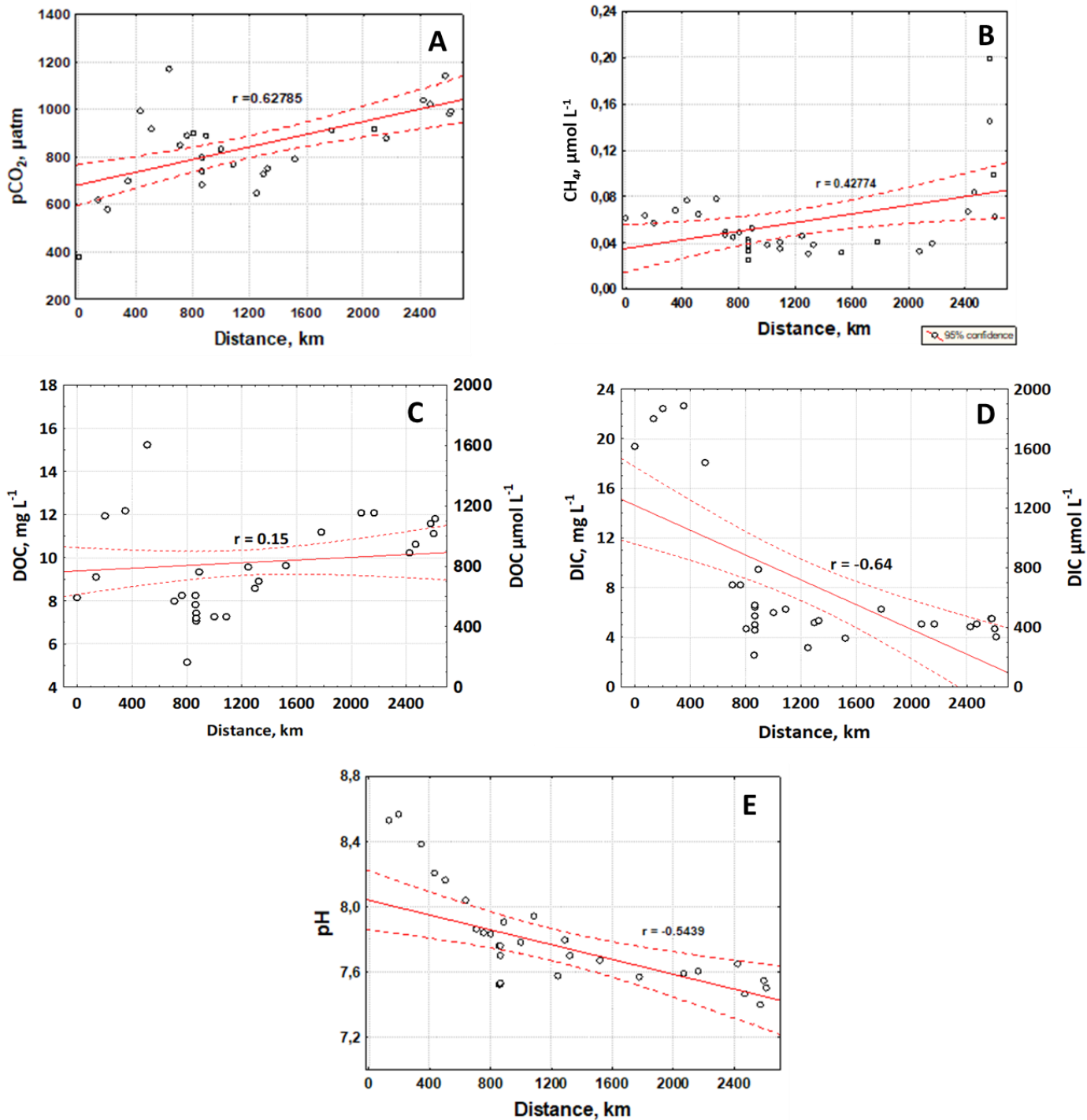
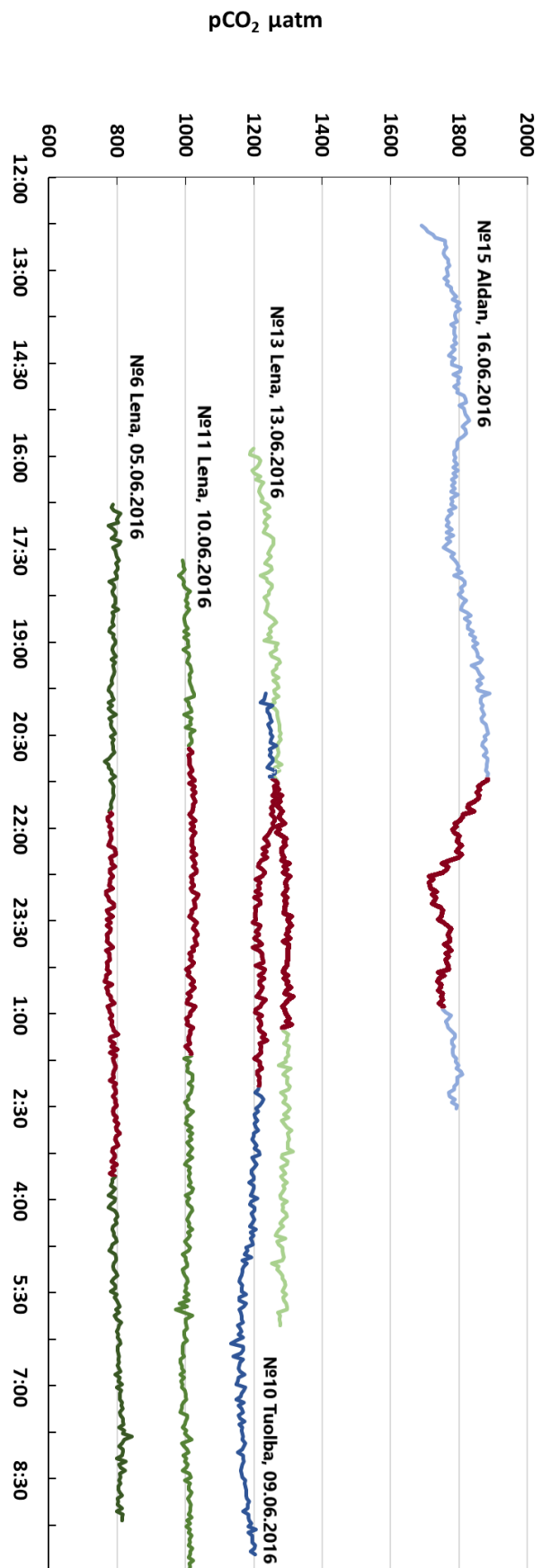


Figure 2. A 20-km averaged pCO_2 profile (A) and calculated CO_2 fluxes (B) of the Lena River main stem of over 2600 km distance, from Zhigalovo to the Tumara River. The average pCO_2 (μatm) and fluxes ($\text{g C m}^{-2} \text{ d}^{-1}$) of the main sampled tributaries are provided as numbers below X axes. Note that peaks of CO_2 concentration at the main stem are not linked to conflux with tributaries.



974
975
976
977
978
979
980
981

Figure 3. Averaged (over 20-km distance) CO_2 (A), CH_4 (B), DOC (C), DIC (D) and pH (E) concentration over the distance of the boat route at the Lena River, from the south-west to north-east.



982

983 **Figure 4.** Continuous pCO₂ concentration in the Lena River and two tributaries from late afternoon to
 984 morning next day. Red part of the line represents night time. Variations of water temperature did not
 985 exceed 2 °C.

986
987
988
989
990
991
992
993
994
995

